

EQUI-CENTRO-AFFINE EXTREMAL HYPERSURFACES IN ELLIPSOID

YUN YANG AND CHANGZHENG QU*

ABSTRACT. This paper explores equi-centro-affine extremal hypersurfaces in an ellipsoid. By analyzing the evolution of invariant submanifold flows under centro-affine unimodular transformations, we derive the first and second variational formulas for the associated invariant area. Stability analysis reveals that the circles with radius $r = \sqrt{6}/3$ on $\mathbb{S}^2(1)$ are characterized as being equi-centro-affine maximal. Furthermore, we provide a detailed classification of the compact isoparametric equi-centro-affine extremal hypersurfaces on $(n+1)$ -dimensional sphere, as well as the generalized closed equi-centro-affine extremal curves on 2-dimensional sphere. These curves are shown to belong to a family of transcendental curves $x_{p,q}$ (p, q are two coprime positive integers satisfying that $1/2 < p/q < 1$). Additionally, we establish an equi-centro-affine version of isoperimetric inequality ${}^e\mathcal{L}^3 \leq (4\pi - A)(2\pi - A)A$ on $\mathbb{S}^2(1)$.

1. INTRODUCTION

In general, minimal submanifolds serve as the critical points of the area or volume functional [4, 5, 21], which also emerge as static solutions of the mean curvature flow [26, 54]. On one hand, minimal submanifolds, occupying a prominent position in global differential geometry, have been studied extensively, yielding a plethora of fascinating results (refer to [7, 8, 10, 11] for novel and significant achievements). On the other hand, various delicate methods such as variational method, Min-Max theory, have been proposed to construct minimal submanifolds [31, 32, 33], and subsequently, the analysis of the second variation can provide valuable insights into the stability, as detailed in [18, 19]. Certainly, the theory of minimal submanifolds, being a pivotal theme in geometric analysis, has been affirmed as a powerful and essential instrument in mathematics [9]. Sustained development addressing innovative and substantial accomplishments in minimal submanifolds, besides being important in its own right, may also greatly enhance potential applications in related disciplines such as computer vision, probability and general relativity. In this paper, we focus on the equi-centro-affine extremal hypersurfaces M^n in an ellipsoid $N^{n+1} \subset \mathbb{R}^{n+2}$.

The problem of finding a minimal surface with a prescribed boundary has engaged such prolific mathematicians as Lagrange and Euler, as well

* Corresponding author: quchangzheng@nbu.edu.cn

2010 *Mathematics Subject Classification.* 53A15, 53A55, 53A10, 58E12.

Key words and phrases. equi-centro-affine geometry; Euler-Lagrange equation; variational formula; isoperimetric inequality.

as, Plateau. It was Plateau who first delved into the study of the surface obtained in the form of a soap film stretched on a wire framework, a physical example of a minimal surface, and this problem has become known as the famous Plateau's problem [22, 23, 38]. Other noteworthy examples of minimal surfaces include helicoids and catenoids [20]. The Bernstein problem also holds a pivotal role in the theory of minimal submanifolds [2, 6], and numerous investigations have emerged focusing on Bernstein type problems in Euclidean spaces (see [24, 40, 43] and the references therein).

A natural generalization is to study minimal surfaces in Riemannian manifolds, deviating from the conventional setting of \mathbb{R}^n , with an interesting instance being the n -dimensional sphere, denoted as \mathbb{S}^n [7, 8, 9, 17]. Note that a crucial distinction from the \mathbb{R}^n scenario lies in the fact that: every minimal submanifold in \mathbb{R}^n inherently possesses a non-compact nature, whereas in \mathbb{S}^n , one can encounter closed minimal submanifolds.

Let M^n be an n -dimensional Riemannian manifold that is immersed isometrically into a space form N^{n+1} with constant curvature c . The immersion's principal curvatures are denoted by $\kappa_1, \dots, \kappa_n$. For r ranging from 0 to n , let S_r represent the r -th elementary symmetric polynomial, which is given by the sum of all possible products of r distinct principal curvatures: $\sum_{i_1 < i_2 < \dots < i_r} \kappa_{i_1} \kappa_{i_2} \dots \kappa_{i_r}$. Reilly [39] extended variational

problems concerning the area or volume functional to any smooth function $f(S_1, \dots, S_n)$ defined on the manifold M^n , specifically integrals of the form $\int_M f(S_1, \dots, S_n) dV$, where dV represents the volume element on M^n .

The Willmore submanifold [12, 29] is an extremal submanifold in terms of the Willmore functional $\int_M (S - nH^2)^{n/2} dV$, where S denotes the square of the length of the second fundamental form, H signifies the mean curvature of M^n . Notably, it remains invariant under Möbius (or conformal) transformations of $\mathbb{S}^{n+1}(1)$.

The variational issue in the affine setting is a little more complicated (refer to [50, 51] for the variational problems respect to the affine arc length). The exploration of affine differential geometry is grounded in the Lie group $A(n, \mathbb{R}) = GL(n, \mathbb{R}) \times \mathbb{R}^n$ which includes affine transformations of the form $x \mapsto Ax + b$, $A \in GL(n, \mathbb{R})$, $b \in \mathbb{R}^n$ acting on $x \in \mathbb{R}^n$ (refer to Nomizu and Sasaki [36] and Simon [42] for details). Analogously, equi-affine geometry is confined to the subgroup $SA(n, \mathbb{R}) = SL(n, \mathbb{R}) \times \mathbb{R}^n$ of volume-preserving affine transformations. Centro-affine differential geometry refers to the subgroup of the affine transformation group that keeps the origin fixed, which is closely related to the geometry induced by the general linear group $x \mapsto Ax$, $A \in GL(n, \mathbb{R})$, $x \in \mathbb{R}^n$. Furthermore, equi-centro-affine differential geometry arises in connection with the subgroup $SL(n, \mathbb{R})$ of volume-preserving linear transformations.

In equi-affine differential geometry, the ambient space \mathbb{R}^{n+2} has a flat affine connection D and the usual determinant function is regarded as a parallel volume element. Let $\mathbf{x} : N^{n+1} \rightarrow \mathbb{R}^{n+2}$ be a local embedding of a smooth hypersurface, and ξ be the affine normal field to \mathbf{x} . The equi-affine structure equations of \mathbf{x} may be written as (see [30, 36] for more details)

$$\begin{aligned}\mathbf{x}_{ij} &= \bar{g}_{ij}\xi + (\bar{\Gamma}_{ij}^k + C_{ij}^k)\mathbf{x}_k, \\ \xi_i &= -A_i^k\mathbf{x}_k,\end{aligned}$$

where \bar{g}_{ij} is the equi-affine metric, $\bar{\Gamma}_{ij}^k$ are the Christoffel symbols of the metric \bar{g}_{ij} , C_{ij}^k is called cubic form, and A_i^k is the equi-affine shape operator.

The Euclidean inner product $\langle \cdot, \cdot \rangle$ on \mathbb{R}^{n+2} induces the metric ${}^e g_{ij}$ and the Euclidean second fundamental form ${}^e h_{ij}$ on \mathbf{x} . According to the literature [30], the connection between the equi-affine and Euclidean metrics is given by

$$\bar{g}_{ij} = \frac{{}^e h_{ij}}{\phi}, \quad (1.1)$$

where $\phi = \left(\frac{\det {}^e h_{ij}}{\det {}^e g_{ij}} \right)^{1/(n+2)}$.

The extremal submanifolds in equi-affine space \mathbb{R}^{n+2} are the critical points of the equi-affine invariant area functional given by $\int_N \sqrt{|\det \bar{g}_{ij}|} d\mu_N$. Note that, commonly in the literature, the term ‘‘affine geometry’’ is used interchangeably with ‘‘equi-affine geometry’’.

In approximately 1977, Chern [16] conjectured that an affine maximal graph of a smooth, locally uniformly convex function on two-dimensional Euclidean space, \mathbb{R}^2 , is necessarily a paraboloid. The two-dimensional Chern’s conjecture was fully resolved by Trudinger and Wang in their celebrated paper [45]. However, the higher-dimensional Bernstein problem remains unsolved. Later, Li and Jia [28], and also Trudinger and Wang [46], proved Calabi’s conjecture for two-dimensions separately, using distinctively different approaches. Additionally, Trudinger and Wang investigated the Plateau problem for affine maximal hypersurfaces, which serves as the analogous affine-invariant counterpart of the classical Plateau problem for minimal surfaces [47]. In [49], Wang declared that the concept of an affine maximal surface in affine geometry mirrors that of minimal surface in Euclidean geometry (Calabi [14] advocated for the terminology ‘‘affine maximal’’ as the second variation of the affine area functional is negative). The affine Bernstein problem and the affine Plateau problem, as introduced in [14, 15, 16], constitute two fundamental issues of affine maximal submanifolds.

In this paper, we explore the equi-centro-affine maximal hypersurfaces M^n immersed in the ellipsoid N^{n+1} which is centered at the origin in \mathbb{R}^{n+2} . Certainly, it is universally acknowledged that an ellipsoid in the equi-affine setting is an affine sphere with vanishing cubic form. Under an equi-affine

transformation, the ellipsoid N^{n+1} may be formulated as

$$\mathbf{x} = R \left\{ \cos r, \sin r \cos \theta^1, \dots, \sin r \sin \theta^1 \dots \sin \theta^{n-1} \cos \theta^n, \right. \\ \left. \sin r \sin \theta^1 \dots \sin \theta^n \right\}. \quad (1.2)$$

where $R = (a_0 a_1 \dots a_{n+1})^{1/(n+2)}$, and a_0, a_1, \dots, a_{n+1} represent the lengths of the semi-axes of the ellipsoid. Denote $\varrho = R^{\frac{n+2}{n+3}}$. Then by (1.1), the equi-affine metric of the ellipsoid \mathbf{x} can be written as

$$\bar{g} = \varrho^2 \begin{pmatrix} 1 & 0 & \dots & 0 \\ 0 & \sin^2 r & \dots & 0 \\ 0 & 0 & \dots & 0 \\ \dots & \dots & \dots & \dots \\ 0 & 0 & \dots & \sin^2 r \sin^2 \theta^1 \dots \sin^2 \theta^{n-1} \end{pmatrix}. \quad (1.3)$$

Since R and ϱ are equal up to a constant scaling factor, it is permissible to interchange ϱ with R in equi-affine metric (1.3) of the ellipsoid N^{n+1} .

Alternatively, M^n is a submanifold of codimension two in \mathbb{R}^{n+2} , endowed with an equi-centro-affine structure, as detailed in [35, 36, 48, 53]. Then for any local oriented basis $\sigma = \{E_1, E_2, \dots, E_n\}$ of TM with dual basis $\{\theta^1, \theta^2, \dots, \theta^n\}$, we introduce the term

$$G := [E_1(x), \dots, E_n(x), x, d^2x] = G_{ij} \theta^i \otimes \theta^j, \quad (1.4)$$

under the assumption that G is nondegenerate, where the bracket notation $[\dots]$ is employed to denote the standard determinant in \mathbb{R}^{n+2} , and

$$G_{ij} := [E_1(x), \dots, E_n(x), x, E_i E_j(x)]$$

is a symmetric 2-form. Moreover, we may verify that

$$\tilde{g} := \tilde{g}_{ij} \theta^i \otimes \theta^j, \quad \tilde{g}_{ij} = |\det(G_{pq})|^{-\frac{1}{n+2}} G_{ij} \quad (1.5)$$

is independent of the choice of the basis σ and thus a globally defined symmetric 2-form, which also is invariant up to the equi-centro-affine transformations in \mathbb{R}^{n+2} . According to [53], $\{\tilde{g}_{ij}\}$ is identified as an equi-centro-affine metric associated with the immersion $\mathbf{x} : M^n \rightarrow \mathbb{R}^{n+2}$. Let $\Delta_{\tilde{g}}$ denote the Laplacian of \tilde{g} . $\{\mathbf{x}, \frac{\Delta_{\tilde{g}} \mathbf{x}}{n}\}$ is characterized as the equi-centro-affine normalization of $\mathbf{x} : M^n \rightarrow \mathbb{R}^{n+2}$.

The focus of the present question shifts to elucidating the extremal equi-centro-affine hypersurfaces of the ellipsoid N^{n+1} endowed with the equi-affine metric in \mathbb{R}^{n+2} , which arise from the application of the equi-centro-affine metric defined on M^n .

Given that M^n is furthermore a submanifold residing in the ellipsoid N^{n+1} centered at origin of \mathbb{R}^{n+2} . The equi-centro-affine invariant area function

$\int_M \sqrt{\det \tilde{g}_{ij}} d\mu_M$ can be denoted by (see Section 2.2)

$$\Sigma_{eca} = \varrho^{\frac{n}{n+2}} \int_M S_n^{\frac{1}{n+2}} \sqrt{\det(g_{ij})} d\mu_M,$$

where g_{ij} is the metric of M^n induced from \bar{g}_{ij} . Note that, as a consequence of the nondegeneracy condition of the metric \tilde{g} , $S_n \neq 0$ holds true on the submanifold M^n . Furthermore, when n takes on an even number, the same nondegeneracy condition ensures that $S_n > 0$. In Section 3.1, we will prove the following theorem:

Theorem 1.1. *The first variational formula, for the equi-centro-affine invariant area of a hypersurface M^n in the ellipsoid N^{n+1} is*

$$\begin{aligned} \frac{d}{dt} \Sigma_{eca} = & \varrho^{\frac{n}{n+2}} \int_M \frac{U}{n+2} \left(T_{n-1}{}^{ij} \nabla_{e_i} \nabla_{e_j} \left(S_n^{-\frac{n+1}{n+2}} \right) \right. \\ & \left. + S_n^{-\frac{n+1}{n+2}} \left(\frac{1}{\varrho^2} S_{n-1} - (n+1) S_n S_1 \right) \right) dV. \end{aligned}$$

Let us denote

$${}^e\mathcal{H} = T_{n-1}{}^{ij} \nabla_{e_i} \nabla_{e_j} \left(S_n^{-\frac{n+1}{n+2}} \right) + S_n^{-\frac{n+1}{n+2}} \left(\frac{1}{\varrho^2} S_{n-1} - (n+1) S_n S_1 \right). \quad (1.6)$$

The hypersurface in the ellipsoid is said to be an equi-centro-affine extremal hypersurface if ${}^e\mathcal{H} = 0$.

Remark 1.2. When $n = 2$ and $R = 1$, ${}^e\mathcal{H} = 0$ reduces to

$$S_1 \left(\Delta_g \left(S_2^{-\frac{3}{4}} \right) + S_2^{-\frac{3}{4}} (1 - 3S_2) \right) = 0,$$

where Δ_g denotes the Laplace-Beltrami operator with respect to metric g of M^n induced from \bar{g} . Since $S_2 > 0$, we conclude that $S_1 \neq 0$. Thus

$$\Delta_g \left(S_2^{-\frac{3}{4}} \right) + S_2^{-\frac{3}{4}} (1 - 3S_2) = 0.$$

The trivial solution for this equation is $S_2 = 1/3$. Assume M^2 is compact, we obtain a Simon's type equality (see [29, 41] for Simon's type integral inequality)

$$\int_M S_2^{-\frac{3}{4}} (1 - 3S_2) dV = 0.$$

Let us draw an analogy with the affine maximal hypersurface in \mathbb{R}^n . If the affine maximal hypersurface M^n in \mathbb{R}^{n+1} can be represented as the graph of a convex function u , then u satisfies the Monge-Ampere type equation $\Delta_{\bar{g}} \left(\det(D^2u)^{-1/(n+2)} \right) = 0$ and $\Delta_{\bar{g}}$ denotes the Laplace-Beltrami operator with respect to equi-affine metric \bar{g} . It is noteworthy that the higher-dimensional affine maximal hypersurface problems remain unsolved to date.

The Clifford type hypersurfaces

$$M^n = \mathbb{S}^m \left(\sqrt{\frac{m+1}{n+2}} \right) \times \mathbb{S}^{n-m} \left(\sqrt{\frac{n+1-m}{n+2}} \right), \quad 1 \leq m \leq n-1$$

are examples of equi-centro-affine extremal hypersurfaces in unit sphere (refer to Section 4 for a comprehensive classification of isoparametric equi-centro-affine extremal hypersurfaces). Under the specified conditions $2m = n$ and m being an even number, the aforementioned Clifford-type hypersurfaces M^n are Euclidean minimal hypersurfaces and also Willmore hypersurfaces.

In Section 3.2, we derive the second variational formula for the equi-centro-affine invariant area of a hypersurface M^n immersed in the ellipsoid N^{n+1} (see Theorem 3.1). Based on this theorem, we embark on an investigation into the stability of curves with respect to the equi-centro-affine arc length when they are considered on the unit sphere $\mathbb{S}^2(1)$. One of our main results is

Theorem 1.3. *On the unit sphere $\mathbb{S}^2(1)$, the circle with radius $r = \frac{\sqrt{6}}{3}$ stands out as a unique embedded closed curve that is simultaneously stable and equi-centro-affine maximal.*

Remark 1.4. According to Theorem 1.3, on $\mathbb{S}^2(1)$, if there exists a maximizer of the equi-centro-affine arc length among all embedded closed curves, then that curve is necessarily a planar circle with radius $r = \sqrt{6}/3$. In this scenario, the equi-centro-affine arc length ${}^e\mathcal{L}$ of any embedded closed curve on $\mathbb{S}^2(1)$ is upper-bounded by ${}^e\mathcal{L} \leq 2^{\frac{4}{3}}\sqrt{3}\pi/3$. Let A denote the area enclosed by an embedded closed curve on open hemisphere of $\mathbb{S}^2(1)$. Assuming further that a maximizer of the equi-centro-affine arc length exists for curves with a fixed enclosed area, Section 3.3.2 and Theorem 5.11 jointly establish a profound equi-centro-affine isoperimetric inequality ${}^e\mathcal{L}^3 \leq (4\pi - A)(2\pi - A)A$, with equality achieved solely by planar circles.

For a closed equi-centro-affine extremal curve on the unit sphere $\mathbb{S}^2(1)$, the progression angle Λ^Θ in one period of the curvature is

$$\Lambda^\Theta = \frac{4}{(a+r)\sqrt{(a-c)}} \Pi \left(\frac{a-b}{a+r}, \frac{\pi}{2}, \frac{a-b}{a-c} \right) - \frac{4}{(a-r)\sqrt{(a-c)}} \Pi \left(\frac{a-b}{a-r}, \frac{\pi}{2}, \frac{a-b}{a-c} \right),$$

where $C_2 > 3\sqrt[3]{4}$, and Π is the elliptic integral of the third kind. Additionally, a, b, c are the three distinct solutions of the cubic polynomial $x^3 - C_2x + 4 = 0$, satisfying the specific ordering $a > b > 0 > c$, and $r = \sqrt{C_2}$. In Appendix B, we will prove that Λ^Θ exhibits monotonic decrease with the increase of the parameter C_2 , and $\pi < \Lambda^\Theta < \sqrt{2}\pi$. In relation to the classification of closed equi-centro-affine extremal curves on the unit sphere \mathbb{S}^2 , we establish

Theorem 1.5. *Let \mathbf{x} be a closed equi-centro-affine extremal curve on the unit sphere $\mathbb{S}^2(1)$. Then we have the following possibilities for \mathbf{x} :*

- (1) \mathbf{x} is a planar circle with radius $\sqrt{6}/3$;
- (2) $\mathbf{x} = \mathbf{x}_{p,q}$ has rotation index p and closes up in q periods of its curvature function. The pair (p, q) is not arbitrary and must be such that p/q is defined in the open interval $(\frac{1}{2}, \frac{\sqrt{2}}{2})$.

The rest of this paper is organized as follows. In Section 2, we review the geometry of equi-affine space and equi-centro-affine space, and deduce the equi-centro-affine invariant area function for the hypersurface M^n immersed in ellipsoid N^{n+1} . Section 3 is dedicated to the computation of variational formulas, specifically focusing on the equi-centro-affine area and arc-length of equi-centro-affine curves residing on the ellipsoid. In Section 4, our attention shifts to the investigation of equi-centro-affine extremal hypersurfaces on the unit sphere. Lastly, in Section 5, the closed equi-centro-affine extremal curves on the sphere are studied. As a conclusion, a classification of closed generalized equi-centro-affine extremal curves on the sphere is presented.

2. PRELIMINARIES

In this section, we undertake a thorough examination of the essential geometric concepts relating to equi-affine and equi-centro-affine spaces. This pivotal understanding acts as the foundation for our subsequent analysis, enabling us to explore the equi-affine invariants on the ellipsoid.

2.1. Ellipsoid with equi-affine metric. Suppose that N^{n+1} is an ellipsoid centered at the origin in \mathbb{R}^{n+2} , and under an equi-affine transformation, it may be expressed in the form given by (1.2). A simple computation yields

$$\begin{aligned} [\mathbf{x}_r, \mathbf{x}_{\theta^1}, \dots, \mathbf{x}_{\theta^n}, \mathbf{x}] &= (-1)^{n+1} a_0 \cdots a_{n+1} \sin^n r \sin^{n-1} \theta^1 \cdots \sin \theta^{n-1} \\ &= (-1)^{n+1} \sqrt{\det \bar{g}}. \end{aligned}$$

Consider the local embedding map

$$\mathbf{x} : \mathbb{S}^n \mapsto M^n \hookrightarrow N^{n+1} \hookrightarrow \mathbb{R}^{n+2},$$

and let D denote the Levi-Civita connection on \mathbb{S}^n . We typically consider $r(\theta^1, \dots, \theta^n)$ as a function defined on the n -sphere \mathbb{S}^n . The derivative of $r(\theta^1, \dots, \theta^n)$ along the direction specified by the partial derivative operator $\frac{\partial}{\partial \theta^i}$ is commonly denoted as $D_i r$.

With this understanding, we can then proceed to define the local coordinate vector fields on the manifold M^n , utilizing these derivatives and the intrinsic structure of \mathbb{S}^n

$$e_i \triangleq \mathbf{x}_* \left(\frac{\partial}{\partial \theta^i} \right) = \frac{\partial \mathbf{x}}{\partial \theta^i} = D_i r \frac{\partial}{\partial r} + \frac{\partial}{\partial \theta^i}, \quad 1 \leq i \leq n, \quad (2.1)$$

and the outward unit normal vector of M^n with respect to the metric \bar{g}

$$\nu = \frac{1}{v} \left(\frac{\partial}{\partial r} - \lambda^{-2}(r) D^j r \frac{\partial}{\partial \theta^j} \right), \quad (2.2)$$

where $\lambda(r) = \sin r$, $D^j r = \sigma^{ij} D_i r$, (σ^{ij}) is the inverse matrix of the metric tensor

$$(\sigma_{ij}) = \begin{pmatrix} 1 & 0 & \cdots & 0 \\ 0 & \sin^2 \theta^1 & \cdots & 0 \\ \cdots & \cdots & \cdots & \cdots \\ 0 & 0 & \cdots & \sin^2 \theta^1 \cdots \sin^2 \theta^{n-1} \end{pmatrix}$$

of \mathbb{S}^n . In addition, $v = \varrho \sqrt{1 + \lambda^{-2}(r) |Dr|^2}$, and $|\cdot|$ is the norm with respect to the metric σ_{ij} .

It is observed that, according to (1.3)

$$\bar{\Gamma}_{ij}^k = \hat{\Gamma}_{ij}^k, \quad \bar{\Gamma}_{ij}^0 = -\lambda \lambda' \sigma_{ij}, \quad \bar{\Gamma}_{0i}^k = \frac{\lambda'}{\lambda} \delta_i^k, \quad \bar{\Gamma}_{0i}^0 = \bar{\Gamma}_{00}^k = \bar{\Gamma}_{00}^0 = 0,$$

where $\hat{\Gamma}_{ij}^k$ denote the Christoffel symbols of \mathbb{S}^n with respect to the tangent basis $\{\frac{\partial}{\partial \theta^i}\}$, $i = 1, \dots, n$ and $\bar{\Gamma}_{\alpha\beta}^\gamma$ denote the Christoffel symbols of N^{n+1} with respect to the metric \bar{g} . Now direct evaluation reveals

$$\begin{aligned} [e_1, e_2, \dots, e_n, \nu, \mathbf{x}] &= \frac{1}{v} [\mathbf{x}_1, \dots, \mathbf{x}_n, \mathbf{x}_r, \mathbf{x}] \begin{vmatrix} 1 & 0 & \cdots & -\frac{r^1}{\lambda^2} & 0 \\ 0 & 1 & \cdots & -\frac{r^2}{\lambda^2} & 0 \\ \cdots & \cdots & \cdots & \cdots & \cdots \\ r_1 & r_2 & \cdots & 1 & 0 \\ 0 & 0 & \cdots & 0 & 1 \end{vmatrix} \\ &= \frac{v}{\varrho^2} [\mathbf{x}_1, \dots, \mathbf{x}_n, \mathbf{x}_r, \mathbf{x}]. \end{aligned}$$

By comparison, we may find

$$\bar{\nabla}_{e_i} e_j = \Gamma_{ij}^k e_k + h_{ij} \nu, \quad \bar{\nabla}_{e_i} \nu = S_i^k e_k,$$

and the metric $g = g_{ij} d\theta^i d\theta^j$ of M^n induced from \bar{g} is

$$g_{ij} = \bar{g}(e_i, e_j) = \varrho^2 r_i r_j + \varrho^2 \lambda^2(r) \sigma_{ij}.$$

Note that in this paper subscripts after a semicolon “;” are used to denote covariant derivatives with respect to the induced equi-affine metric g_{ij} . Unless otherwise noted, we raise and lower indices using the metric g_{ij} .

Through direct computations, we arrive at

$$[e_1, e_2, \dots, e_n, \nu, \mathbf{x}] = -\varrho \sqrt{\det(g_{ij})}$$

and

$$h_{ij} = g(\bar{\nabla}_{e_i} e_j, \nu) = \frac{\varrho^2}{v} \left(r_{i;j} - \lambda(r) \lambda'(r) \sigma_{ij} - 2 \frac{\lambda'(r)}{\lambda(r)} r_i r_j \right),$$

where $r_{i;j}$ denotes the second covariant derivative of r with respect to the Christoffel symbols $\hat{\Gamma}_{ij}^k$.

Let S_r denote the r -th elementary symmetric function of the the eigenvalues k_1, \dots, k_n of h , specifically:

$$S_0 = 1, S_1 = k_1 + \dots + k_n, \dots, S_n = k_1 \dots k_n.$$

The Newton transformation T_r are then defined inductively in the following manner

$$T_{0j}^i = \delta_j^i, T_{r+1j}^i = S_{r+1} \delta_j^i - T_r^{ik} h_{kj}, r = 0, 1, \dots, n-1,$$

where δ_j^i is the Kronecker delta function.

2.2. Equi-centro-affine hypersurfaces in ellipsoid. Let N^{n+1} be an ellipsoid, centered at the origin in \mathbb{R}^{n+2} , equipped with the equi-affine metric that is precisely specified in (1.2) and (1.3). Given the map

$$\mathbf{x} : \mathbb{S}^n \mapsto M^n \hookrightarrow N^{n+1},$$

where M^n is smoothly immersed in the ellipsoid N^{n+1} , and the metric on M^n is the equi-centro-affine metric as defined in (1.5). Utilizing the relations established in (1.4) and (1.5), we proceed with the following derivation

$$\begin{aligned} G_{ij} &= [e_1, \dots, e_n, \mathbf{x}, \bar{\nabla}_{e_i} e_j] \\ &= h_{ij} [e_1, e_2, \dots, e_n, \mathbf{x}, \nu] = h_{ij} \varrho \sqrt{\det(g_{ij})}. \end{aligned}$$

Moreover,

$$\tilde{g}_{ij} = \varrho^{\frac{2}{n+2}} (\det(g_{ij}))^{\frac{1}{n+2}} (\det(h_{ij}))^{-\frac{1}{n+2}} h_{ij} = \varrho^{\frac{2}{n+2}} S_n^{-\frac{1}{n+2}} h_{ij},$$

and

$$\det(\tilde{g}_{ij}) = \varrho^{\frac{2n}{n+2}} S_n^{\frac{2}{n+2}} \det(g_{ij}).$$

Throughout the paper, we consistently assume that $S_n \neq 0$ on M^n , and further, when n is an even number, we impose the condition $S_n > 0$. Consequently, the equi-centro-affine invariant area function with respect to the metric \tilde{g} may be formulated as

$$\Sigma_{eca} = \varrho^{\frac{n}{n+2}} \int_M S_n^{\frac{1}{n+2}} \sqrt{\det(g_{ij})} d\mu.$$

3. THE VARIATIONAL FORMULAS

3.1. The proof of Theorem 1.1. Suppose that $N^{n+1} \subset \mathbb{R}^{n+2}$ is an ellipsoid endowed with the equi-affine metric as specified in (1.2) and (1.3). Let $\mathbf{x}(\cdot, t) : \mathbb{S}^n \rightarrow M^n \hookrightarrow N^{n+1}$ represent a smooth one-parameter family of hypersurface immersions evolving in N^{n+1} . We aim to consider the invariant hypersurface flow in N^{n+1}

$$\frac{\partial \mathbf{x}}{\partial t} = W^k e_k + U \nu, \quad (3.1)$$

where W^k are some $(1, 0)$ tensors, U is equi-centro-affine invariant, and e_k and ν are defined in (2.1) and (2.2). Here, the term ‘‘invariant hypersurface

flow" refers to motions of the hypersurface \mathbf{x} governed by (3.1), which possess the property of being invariant under the action of the equi-centro-affine transformation group in \mathbb{R}^{n+2} . In view of the computation in [39], we have

$$\begin{aligned}\frac{\partial g_{ij}}{\partial t} &= -2Uh_{ij} + W_{j,i} + W_{i,j}, \\ \frac{\partial h_{ij}}{\partial t} &= U_{,ij} - Uh_{im}h_j^m + W_{,i}^k h_{kj} + W_{,j}^k h_{ki} + W^k h_{kij} + \frac{U}{\varrho^2} g_{ij}, \\ \frac{\partial \nu}{\partial t} &= -(U_i + W^l h_{il}) g^{ij} e_j.\end{aligned}$$

Let $g = \det(g_{ij})$. It is easy to verify that

$$\frac{1}{g} \frac{\partial g}{\partial t} = -2 \left(S_1 U - W_{,j}^j \right),$$

and

$$\begin{aligned}\frac{\partial S_r}{\partial t} &= U(S_1 S_r - (r+1)S_{r+1}) + T_{r-1}^{ij} U_{,ij} \\ &\quad + S_{r,j} W^j + \frac{U}{\varrho^2} (n-r+1) S_r.\end{aligned}\tag{3.2}$$

Consider the deformations \mathbf{x} in (3.1) which leave ∂M^n strongly fixed in the sense that both U and its gradient vanish on ∂M^n . It follows that if M^n is compact and ∂M^n is empty, then there is no restriction on the deformation. The formula for the first variation with fixed boundary of the equi-centro-affine area integral for a hypersurface in an ellipsoid is

$$\begin{aligned}\frac{d}{dt} \Sigma_{eca} &= \varrho^{\frac{n}{n+2}} \int_M \frac{U}{n+2} \left(T_{n-1}^{ij} \nabla_{e_i} \nabla_{e_j} \left(S_n^{-\frac{n+1}{n+2}} \right) \right. \\ &\quad \left. + S_n^{-\frac{n+1}{n+2}} \left(\frac{1}{\varrho^2} S_{n-1} - (n+1) S_n S_1 \right) \right) dV.\end{aligned}\tag{3.3}$$

Hence, we have successfully completed the proof of Theorem 1.1.

3.2. The second variational formula. Let us direct our concentration towards the second variation. Firstly, we may obtain

$$\frac{\partial \Gamma_{ij}^k}{\partial t} = g^{kl} (U_l h_{ij} - U_j h_{il} - U_i h_{jl} - U h_{ijl}) + W_{,ij}^k - W^m R_{ijm}^k.\tag{3.4}$$

In [39], it is explicitly stated that $T_n = 0$, $T_{r+1} = S_{r+1} I - AT_r$, and $T_r A = AT_r$, which implies

$$\begin{aligned}\frac{\partial T_{n-1}^{ij}}{\partial t} &= U_{,mk} \left(T_{n-1}^{ij} b^{mk} - T_{n-1}^{mi} b^{jk} \right) \\ &\quad + U \left(S_1 T_{n-1}^{ij} + S_n g^{ij} + \frac{1}{\varrho^2} T_{n-2}^{ij} \right) \\ &\quad + W^k T_{n-1,k}^{ij} - \left(W_{,k}^j T_{n-1}^{ki} + W_{,k}^i T_{n-1}^{kj} \right),\end{aligned}\tag{3.5}$$

where A is the matrix (h_{ij}) , and (b^{ij}) is the inverse matrix of (h_{ij}) . Upon utilizing (3.4), (3.5), and (3.3), and engaging in a non-trivial calculation process (detailed in Appendix A for completeness), we are able to formulate and present the following theorem.

Theorem 3.1. *The second variational formula at the critic point $t = t_0$ is*

$$\begin{aligned} \frac{d^2}{dt^2} \Sigma_{eca}(t_0) = & \frac{\varrho^{\frac{n}{n+2}}}{n+2} \int_M U \left(f^{mkij} U_{,mkij} + f^{mkj} U_{,mkj} \right. \\ & \left. + f^{mk} U_{,mk} + f^m U_{,m} + f U \right) dV, \end{aligned} \quad (3.6)$$

where

$$\begin{aligned} f^{mkij} &= -\frac{n+1}{n+2} S_n^{-\frac{2n+3}{n+2}} T_{n-1}^{ij} T_{n-1}^{mk}, \\ f^{mkj} &= -\frac{2(n+1)}{n+2} \left(S_n^{-\frac{2n+3}{n+1}} T_{n-1}^{mk} \right)_{,i} T_{n-1}^{ij}, \\ f^{mk} &= \left(S_n^{-\frac{n+1}{n+2}} \right)_{,ij} \left(T_{n-1}^{ij} b^{mk} - T_{n-1}^{mi} b^{jk} \right) - \frac{n+1}{n+2} \left(S_n^{-\frac{2n+3}{n+2}} T_{n-1}^{mk} \right)_{,ij} T_{n-1}^{ij} \\ &\quad - \frac{n+1}{n+2} S_n^{-\frac{2n+3}{n+2}} T_{n-1}^{mk} \left(\frac{2}{\varrho^2} S_{n-1} - n S_1 S_n \right) \\ &\quad + S_n^{-\frac{n+1}{n+2}} \left(\frac{1}{\varrho^2} T_{n-1}^{mk} - (n+1)(T_0^{mk} S_n + S_1 T_{n-1}^{mk}) \right), \\ f^m &= -\frac{2(n+1)}{n+2} \left(S_n^{-\frac{2n+3}{n+2}} (S_1 S_n + \frac{1}{\varrho^2} S_{n-1}) \right)_k T_{n-1}^{mk} \\ &\quad + (n-2)(n+1) g^{mk} \left(S_n^{-\frac{1}{n+2}} \right)_k, \\ f &= \left(S_n^{-\frac{n+1}{n+2}} \right)_{,ij} \left(S_1 T_{n-1}^{ij} + S_n g^{ij} + \frac{1}{\varrho^2} T_{n-2}^{ij} \right) + g^{kl} h_{lij} \left(S_n^{-\frac{n+1}{n+2}} \right)_k T_{n-1}^{ij} \\ &\quad - \frac{n+1}{n+2} \left(S_n^{-\frac{2n+3}{n+2}} (S_1 S_n + \frac{1}{\varrho^2} S_{n-1}) \right)_{,ij} T_{n-1}^{ij} \\ &\quad - \frac{n+1}{n+2} S_n^{-\frac{2n+3}{n+2}} \left(\frac{1}{\varrho^4} S_{n-1}^2 - (n+1) S_1^2 S_n^2 - \frac{n}{\varrho^2} S_1 S_{n-1} S_n \right) \\ &\quad + S_n^{-\frac{n+1}{n+2}} \left(\frac{2}{\varrho^4} S_{n-2} - \frac{n}{\varrho^2} S_n + 2(n+1) S_2 S_n \right. \\ &\quad \left. - \frac{n(n+1)}{\varrho^2} S_n - 2(n+1) S_1^2 S_n - \frac{n}{\varrho^2} S_1 S_{n-1} \right). \end{aligned}$$

3.3. Equi-centro-affine curves on ellipsoid. For an ellipsoid N^2 in \mathbb{R}^3 , an equi-affine transformation can be applied to transform it into a sphere centered precisely at the origin, with a radius denoted by R . Since R and ϱ differ only by a constant scaling factor, we henceforth adopt the convention

of substituting R for ϱ in the equi-affine metric (1.3) that characterizes the ellipsoid N^2 .

Consequently, when a curve $\mathbf{x}(p)$ is situated on this transformed spherical surface \mathbb{S}^2 , the quantity $S_1 = k_g$ directly corresponds to the geodesic curvature of the curve \mathbf{x} . This substitution simplifies our analysis and allows us to directly relate the geometric properties of the curve to those of the equivalent spherical surface.

On the spherical surface \mathbb{S}^2 , a vector field \mathbf{J} is designated as a Killing vector field along \mathbf{x} if and only if it satisfies the following conditions (for a detailed discussion, refer to [3, 27]):

$$\begin{aligned} \langle \nabla_{\mathbf{T}} \mathbf{J}, \mathbf{T} \rangle &= 0, \\ \langle \nabla_{\mathbf{T}}^2 \mathbf{J}, \boldsymbol{\epsilon} \rangle + \frac{1}{R^2} \langle \mathbf{J}, \boldsymbol{\epsilon} \rangle &= 0, \end{aligned} \quad (3.7)$$

where $\mathbf{T} = (e/\sqrt{g(e, e)})$ represents the unit tangent vector to the curve, with e is defined as in (2.1), and $\boldsymbol{\epsilon} = \nu$ in (2.2).

3.3.1. *The variational formulations of the equi-centro-affine arc length.* By utilizing (3.3), the first equi-centro-affine variational formula for the curves on the sphere \mathbb{S}^2 may be elegantly expressed as

$${}^{e\mathcal{C}}L'(t) = \frac{1}{3} R^{1/3} \int_{s_1}^{s_2} U \left(B_{ss} - 2B^{-2} + \frac{B}{R^2} \right) ds, \quad (3.8)$$

where $B = (\kappa_g)^{-2/3}$, and $ds = \sqrt{g(e, e)} dp$. At the critical point t_0 , $B_{ss} - 2B^{-2} + BR^{-2} = 0$ holds. Specifically, according to (3.6), the second variational formula is given by

$${}^{e\mathcal{C}}L''(t_0) = \frac{1}{3} R^{1/3} \int_{s_1}^{s_2} U (f_4 U_{ssss} + f_3 U_{sss} + f_2 U_{ss} + f_1 U_s + f_0 U) ds,$$

where

$$\begin{aligned} f_0 &= \frac{1}{R^4} B^{\frac{5}{2}} - \frac{5}{2R^2} B^{\frac{1}{2}} B_s^2 - \frac{9}{R^2} B^{-\frac{1}{2}} - 2B^{-\frac{5}{2}} B_s^2 + 2B^{-\frac{7}{2}}, \\ f_1 &= -\frac{10}{3R^2} B^{\frac{3}{2}} B_s + \frac{5}{3} B^{-\frac{3}{2}} B_s, \quad f_3 = -\frac{10}{3} B^{\frac{3}{2}} B_s, \\ f_2 &= -\frac{5}{2} B^{\frac{1}{2}} B_s^2 + \frac{1}{3R^2} B^{\frac{5}{2}} - \frac{20}{3} B^{-\frac{1}{2}}, \quad f_4 = -\frac{2}{3} B^{\frac{5}{2}}. \end{aligned}$$

Integration by parts gives

$$\begin{aligned}\int_{s_1}^{s_2} f_4 U U_{ssss} ds &= \int_{s_1}^{s_2} \left(f_4 U_{ss}^2 - 2(f_4)_{ss} U_s^2 + \frac{1}{2}(f_4)_{ssss} U^2 \right) ds, \\ \int_{s_1}^{s_2} f_3 U U_{sss} ds &= \int_{s_1}^{s_2} \left(\frac{3}{2}(f_3)_s U_s^2 - \frac{1}{2}(f_3)_{sss} U^2 \right) ds, \\ \int_{s_1}^{s_2} f_2 U U_{ss} ds &= \int_{s_1}^{s_2} \left(-f_2 U_s^2 + \frac{1}{2}(f_2)_{ss} U^2 \right) ds, \\ \int_{s_1}^{s_2} f_1 U U_s ds &= \int_{s_1}^{s_2} -\frac{1}{2}(f_1)_s U^2 ds.\end{aligned}$$

Then one obtains

$${}^e \mathcal{L}''(t_0) = \frac{1}{3} R^{1/3} \int_{s_1}^{s_2} (P_2 U_{ss}^2 + P_1 U_s^2 + P_0 U^2) ds, \quad (3.9)$$

where

$$\begin{aligned}P_0 &= \frac{1}{2}(f_4)_{ssss} - \frac{1}{2}(f_3)_{sss} + \frac{1}{2}(f_2)_{ss} - \frac{1}{2}(f_1)_s + f_0, \\ P_1 &= -2(f_4)_{ss} + \frac{3}{2}(f_3)_s - f_2, \quad P_2 = f_4.\end{aligned}$$

Hence, we have

$$\begin{aligned}P_0 &= \frac{1}{R^4} B^{\frac{5}{2}} - \frac{5}{2R^2} B^{\frac{1}{2}} B_s^2 - \frac{9}{R^2} B^{-\frac{1}{2}} - 2B^{-\frac{5}{2}} B_s^2 + 2B^{-\frac{7}{2}}, \\ P_1 &= \frac{4}{3R^2} B^{\frac{5}{2}} + \frac{10}{3} B^{-\frac{1}{2}}, \quad P_2 = -\frac{2}{3} B^{\frac{5}{2}}.\end{aligned}$$

Solitons of the geometric flow represent self-similar solutions that maintain their shape under the evolution induced by the flow. To formulate the definition of a soliton, let N^n be a n -dimensional Riemannian manifold with metric g , equipped with a Killing vector field \mathbf{J} related to an isometry group $\varphi : N \times \mathbb{R} \rightarrow N$. The isometry group φ characterizes transformations that preserve the metric g and hence the geometric properties of the manifold. The relationship between \mathbf{J} and φ is given by the following differential equation and initial condition

$$\begin{aligned}\frac{d\varphi(x, t)}{dt} &= \mathbf{J}(\varphi(x, t)), \\ \varphi(x, 0) &= x.\end{aligned}$$

Here, $\frac{d\varphi(x, t)}{dt}$ denotes the time derivative of the point $\varphi(x, t)$ in the direction of the flow induced by the Killing vector field \mathbf{J} . The initial condition $\varphi(x, 0) = x$ signifies that at time $t = 0$, the isometry group leaves each point x in N^n unchanged.

A curve \mathbf{x} on N^n is a soliton of the geometric flow (3.1) if, under the action of the isometry group φ parameterized by the flow induced by \mathbf{J} , the curve

evolves in such a way that its shape remains constant up to reparametrization. This property ensures that the soliton maintains its geometric characteristics throughout the evolution process.

Theorem 3.2. *If $U = a(t) \cos \frac{2\pi s}{e\mathcal{L}(t)} + b(t) \sin \frac{2\pi s}{e\mathcal{L}(t)}$ and $W_s = \kappa_g U$ in (3.1), then the closed curve \mathbf{x} is the soliton of the flow (3.1) if and only if its geodesic curvature remains constant. Here $e\mathcal{L}(t)$ represents the Euclidean arc length of \mathbf{x} .*

Proof. If κ_g of the closed curve \mathbf{x} is constant, we can confirm that the vector field $U\epsilon + W\mathbf{T}$ constitutes a Killing vector field for \mathbf{x} by satisfying the conditions outlined in (3.7). \square

Theorem 3.3. *A closed curve with a geodesic curvature of $\kappa_g = \frac{\sqrt{2}}{2R}$ is an equi-centro-affine maximal curve that lies on a sphere, where R represents the radius of the sphere.*

Proof. Given that the geodesic curvature $\kappa_g = \frac{\sqrt{2}}{2R}$, it follows that the curve is a closed planar circle with a radius of $r = \frac{\sqrt{6}}{3}R$. Then by (3.8) and (3.9), at the critic point $t = t_0$, we have

$${}^{e\mathcal{L}}(t_0) = 0$$

and

$$\begin{aligned} {}^{e\mathcal{L}''}(t_0) &= \frac{2^{\frac{5}{6}}}{3}R^2 \int_0^{\frac{2\sqrt{6}\pi}{3}R} \left(-\frac{2}{3}U_{ss}^2 + 3R^{-2}U_s^2 - 3R^{-4}U^2 \right) ds \\ &= -\frac{2^{\frac{5}{6}}\sqrt{6}}{6R} \int_0^{2\pi} (U_{xx}^2 - 3U_x^2 + 2U^2) dx. \end{aligned}$$

Let

$$U = \frac{a_0}{2} + \sum_{m=1}^{\infty} (a_m \cos(mx) + b_m \sin(mx)).$$

According to Theorem 3.2, if the function U is expressed as $U = a \cos(x) + b \sin(x)$, then the resulting closed curves on the sphere with a constant geodesic curvature κ_g are identified as solitons of the given equation (3.1). Consequently, we proceed under the assumption that $a_0, a_2, b_2, a_3, b_3, \dots$ are not all zeros. Then

$$\begin{aligned} \int_0^{2\pi} U^2 dx &= \frac{a_0^2}{2}\pi + \sum_{m=0}^{\infty} (a_m^2 + b_m^2)\pi, \\ \int_0^{2\pi} U_x^2 dx &= \sum_{m=1}^{\infty} m^2 (a_m^2 + b_m^2)\pi, \\ \int_0^{2\pi} U_{xx}^2 dx &= \sum_{m=1}^{\infty} m^4 (a_m^2 + b_m^2)\pi, \end{aligned}$$

which imply

$${}^e\mathcal{L}''(t_0) = -\frac{2^{\frac{5}{6}}\sqrt{6}}{6R} \left(a_0^2\pi + \pi \sum_{m=1}^{\infty} (m^2 - 2)(m^2 - 1)(a_m^2 + b_m^2) \right).$$

Since m is an integer, $(m^2 - 2)(m^2 - 1) \geq 0$. Thus

$${}^e\mathcal{L}''(t_0) < 0.$$

Thus the theorem is proved. \square

3.3.2. The area-fixed variational formulation. On the sphere, let us consider a closed curve denoted by \mathbf{x} , which possesses an Euclidean arc length \mathcal{L} . Furthermore, let A represent the area enclosed by this curve \mathbf{x} . According to the Gauss-Bonnet Theorem, we have the following fundamental relationship

$$\frac{1}{R^2}A + \int_0^{\mathcal{L}} \kappa_g ds = 2\pi.$$

Assuming that the motion governed by (3.1) is area-preserving, a crucial consequence arises from the conservation of enclosed area. Specifically,

$$\frac{d}{dt} \int_0^{\mathcal{L}} \kappa_g ds = 0.$$

According to (3.2), the above equation implies

$$\int_0^{\mathcal{L}} U ds = 0.$$

By (3.8), at the critic point $t = t_0$,

$$\int_0^{\mathcal{L}} U \left(B_{ss} - 2B^{-2} + \frac{B}{R^2} \right) ds = 0.$$

Let us denote

$$C_1 = \int_0^{\mathcal{L}} \left(B_{ss} - 2B^{-2} + \frac{B}{R^2} \right) ds = \int_0^{\mathcal{L}} \left(\frac{B}{R^2} - 2B^{-2} \right) ds.$$

Clearly,

$$\int_0^{\mathcal{L}} C_1 U ds = 0,$$

and

$$\int_0^{\mathcal{L}} U \left(B_{ss} - 2B^{-2} + \frac{B}{R^2} - \frac{C_1}{\mathcal{L}} \right) ds = 0. \quad (3.10)$$

Of course,

$$\int_0^{\mathcal{L}} \left(B_{ss} - 2B^{-2} + \frac{B}{R^2} - \frac{C_1}{\mathcal{L}} \right) ds = 0.$$

If $U = B_{ss} - 2B^{-2} + \frac{B}{R^2} - \frac{C_1}{\ell}$, substituting it into (3.10) yields

$$B_{ss} - 2B^{-2} + \frac{B}{R^2} = \frac{C_1}{\ell},$$

which signifies that the expression $B_{ss} - 2B^{-2} + \frac{B}{R^2}$ is constant.

Let us now delve into the analysis of the stability of the variational formulation, under the assumption that B remains constant. Under this condition, the configuration of \mathbf{x} adopts the shape of a planar circle, with a radius r given by $r = \frac{1}{\sqrt{R^{-2} + B^{-3}}}$. Furthermore, the circumference ℓL of this circle is simply $\ell L = 2r\pi$.

Theorem 3.4. *If B is constant and within the range $\frac{7}{5}R^2 \leq B^3 \leq 2R^2$, then \mathbf{x} is an equi-centro-affine maximal curve on the sphere under the constraint of area-preserving motions.*

Proof. If B is constant, then

$$\begin{aligned} {}^e\mathcal{L}''(t_0) &= \frac{1}{3}R^{\frac{1}{3}} \int_0^{2r\pi} \left(-\frac{2}{3}B^{\frac{5}{2}}U_{ss}^2 + \left(\frac{4}{3R^2}B^{\frac{5}{2}} + \frac{10}{3}B^{-\frac{1}{2}} \right) U_s^2 \right. \\ &\quad \left. + \left(\frac{1}{R^4}B^{\frac{5}{2}} - \frac{9}{R^2}B^{-\frac{1}{2}} + 2B^{-\frac{7}{2}} \right) U^2 \right) ds \\ &= \frac{r}{3}R^{\frac{1}{3}} \int_0^{2\pi} \left(-\frac{2}{3r^4}B^{\frac{5}{2}}U_{xx}^2 + \left(\frac{4}{3r^2R^2}B^{\frac{5}{2}} + \frac{10}{3r^2}B^{-\frac{1}{2}} \right) U_x^2 \right. \\ &\quad \left. + \left(\frac{1}{R^4}B^{\frac{5}{2}} - \frac{9}{R^2}B^{-\frac{1}{2}} + 2B^{-\frac{7}{2}} \right) U^2 \right) dx \\ &= -\frac{r}{9}R^{\frac{1}{3}} \int_0^{2\pi} \left(\frac{1}{R^4}B^{\frac{5}{2}} (2U_{xx}^2 - 4U_x^2 - 3U^2) \right. \\ &\quad \left. + \frac{1}{R^2}B^{-\frac{1}{2}} (4U_{xx}^2 - 14U_x^2 + 27U^2) \right. \\ &\quad \left. + B^{-\frac{7}{2}} (2U_{xx}^2 - 10U_x^2 - 6U^2) \right) dx. \end{aligned}$$

Since $\int_0^{2r\pi} U ds = 0$, we denote U by

$$U = \sum_{m=1}^{\infty} (a_m \cos(mx) + b_m \sin(mx)),$$

where $a_2, b_2, a_3, b_3, \dots$ are not all zeros.

Thus,

$$\begin{aligned} {}^e\mathcal{L}''(t_0) &= -\frac{r}{9}R^{\frac{1}{3}}B^{-\frac{7}{2}} \sum_{m=1}^{\infty} \left((2m^4 - 4m^2 - 3) \frac{B^6}{R^4} \right. \\ &\quad \left. + (4m^4 - 14m^2 + 27) \frac{B^3}{R^2} \right. \\ &\quad \left. + (2m^4 - 10m^2 - 6) \right) (a_m^2 + b_m^2) \pi. \end{aligned}$$

when $m > 2$, we may verify $2m^4 - 4m^2 - 3 > 0$, $4m^4 - 14m^2 + 27 > 0$ and $2m^4 - 10m^2 - 6 > 0$. Conversely, if $m = 1$ (or $m = 2$), by $\frac{7}{5}R^2 \leq B^3 \leq 2R^2$, we see

$$(2m^4 - 4m^2 - 3)\frac{B^6}{R^4} + (4m^4 - 14m^2 + 27)\frac{B^3}{R^2} + (2m^4 - 10m^2 - 6) \geq 0 (> 0).$$

Therefore, we obtain

$${}^e\mathcal{L}''(t_0) < 0.$$

This proves the theorem. \square

4. EQUI-CENTRO-AFFINE EXTREMAL HYPERSURFACES IN UNIT SPHERE

Li [29] derived the isoparametric Willmore hypersurfaces. In a similar fashion, we are tasked with classifying the isoparametric equi-centro-affine extremal hypersurfaces. The subsequent lemma, which serves as a crucial foundation for our classification, was initially presented in [29] (refer to [1, 29, 34, 44] for further details).

Lemma 4.1 ([29]). *Let M be an n -dimensional compact isoparametric hypersurface (i.e. hypersurface with constant principal curvatures) in $\mathbb{S}^{n+1}(1)$. Let $k_1 > k_2 > \cdots > k_g$ be the distinct principal curvatures with multiplicities m_1, m_2, \dots, m_g (so that $n = m_1 + m_2 + \cdots + m_g$). Then*

- (1) g is either 1, 2, 3, 4, or 6.
- (2) If $g = 1$, M is totally umbilic.
- (3) If $g = 2$, $M = \mathbb{S}^m(r_1) \times \mathbb{S}^{n-m}(r_2)$, $r_1^2 + r_2^2 = 1$.
- (4) If $g = 3$, $m_1 = m_2 = m_3 = 2^k$, ($k = 0, 1, 2, 3$).
- (5) If $g = 4$, $m_1 = m_3$ and $m_2 = m_4$. Moreover, $(m_1, m_2) = (2, 2)$ or $(4, 5)$, or $m_1 + m_2 + 1$ is a multiple of $2^{\phi(m_1-1)}$. Here $\phi(l)$ is the number of integers s with $1 \leq s \leq l$ and $s = 0, 1, 2, 4 \pmod{8}$.
- (6) If $g = 6$, $m_1 = m_2 = \cdots = m_6 = 1$ or 2.
- (7) There exists an angle θ , $0 < \theta < \frac{\pi}{g}$ such that

$$k_\alpha = \cot\left(\theta + \frac{\alpha-1}{g}\pi\right), \quad \alpha = 1, 2, \dots, g. \quad (4.1)$$

Initially, leveraging (1.6), we deduce the ensuing result.

Lemma 4.2. *Let M be an n -dimensional equi-centro-affine extremal hypersurface in \mathbb{S}^{n+1} characterized by a constant value of S_n . Then, the following fundamental identity holds:*

$$S_{n-1} - (n+1)S_n S_1 = 0. \quad (4.2)$$

Theorem 4.3. *Let M be an n -dimensional compact isoparametric equi-centro-affine extremal hypersurface in \mathbb{S}^{n+1} . Then the classification of such hypersurfaces, based on their number g of distinct principal curvatures, is as follows:*

(i) If $g = 1$, M is totally umbilic. Specifically, the principal curvatures satisfy $k^2 = \frac{1}{n+1}$ and the radius is $\sqrt{\frac{n+1}{n+2}}$.

(ii) If $g = 2$, M is given by

$$M = \mathbb{S}^m \left(\sqrt{\frac{m+1}{n+2}} \right) \times \mathbb{S}^{n-m} \left(\sqrt{\frac{n+1-m}{n+2}} \right), \quad (4.3)$$

where $1 \leq m \leq n-1$. In particular, if $n = 2m$, and m should be an even number.

(iii) If $g = 3$, the principal curvatures k_1, k_2, k_3 satisfy:

$$\begin{aligned} k_1^2 k_2^2 k_3^2 &= \frac{1}{n+1}, \\ k_1^2 + k_2^2 + k_3^2 &= \frac{3(2n+5)}{n+1}, \\ k_1^2 k_2^2 + k_2^2 k_3^2 + k_1^2 k_3^2 &= \frac{3(3n+5)}{n+1}, \end{aligned}$$

and the dimension n can only take the values $\{3, 6, 12, 24\}$.

(iv) If $g = 4$, the principal curvatures k_1, k_2, k_3, k_4 satisfy:

$$\begin{aligned} k_1 &= 1 + \sqrt{2}, & k_2 &= \sqrt{2} - 1, \\ k_3 &= 1 - \sqrt{2}, & k_4 &= -(1 + \sqrt{2}), \end{aligned}$$

and the dimension n is uniquely determined to be 8.

(v) If $g = 6$, the principal curvatures k_1, \dots, k_6 satisfy:

$$\begin{aligned} k_1 &= 2 + \sqrt{3}, & k_2 &= 1, & k_3 &= 2 - \sqrt{3}, \\ k_4 &= -(2 - \sqrt{3}), & k_5 &= -1, & k_6 &= -(2 + \sqrt{3}), \end{aligned}$$

and the dimension n is fixed at 12.

Proof. (i) If $g = 1$, we have

$$nk_1^{n-1} - n(n+1)k_1^{n+1} = 0,$$

which implies

$$k_1^2 = \frac{1}{n+1}.$$

(ii) If $g = 2$, let distinct principal curvatures are k_1 (multiplicity m) and k_2 (multiplicity $n-m$). Then by (3) of Lemma 4.1, (4.1) and (4.2), we have

$$1 + k_1 k_2 = 0,$$

$$(n-m)k_1^m k_2^{n-m-1} + m k_1^{m-1} k_2^{n-m} - (n+1)k_1^m k_2^{n-m} (m k_1 + (n-m)k_2) = 0.$$

It follows that

$$k_1^2 = \frac{n+1-m}{m+1}.$$

$$\begin{aligned}
M &= \mathbb{S}^m \left(\frac{1}{\sqrt{1+k_1^2}} \right) \times \mathbb{S}^{n-m} \left(\frac{1}{\sqrt{1+\frac{1}{k_1^2}}} \right) \\
&= \mathbb{S}^m \left(\sqrt{\frac{m+1}{n+2}} \right) \times \mathbb{S}^{n-m} \left(\sqrt{\frac{n+1-m}{n+2}} \right),
\end{aligned}$$

where $1 \leq m \leq n-1$.

(iii) If $g = 3$, by (4) of Lemma 4.1, $m_1 = m_2 = m_3 := m$, $n = 3m$. From (7) of Lemma 4.1, we may deduce

$$k_1 = \cot \theta, \quad k_2 = \frac{k_1 - \sqrt{3}}{1 + \sqrt{3}k_1}, \quad k_3 = \frac{k_1 + \sqrt{3}}{1 - \sqrt{3}k_1}.$$

Then

$$(3m+1)k_1^6 - 3(6m+5)k_1^4 + 3(9m+5)k_1^2 - 1 = 0. \quad (4.4)$$

It is direct to confirm that k_2 and k_3 are likewise solutions of (4.4). Hence,

$$\begin{aligned}
k_1^2 k_2^2 k_3^2 &= \frac{1}{n+1}, \\
k_1^2 + k_2^2 + k_3^2 &= \frac{3(2n+5)}{n+1}, \\
k_1^2 k_2^2 + k_2^2 k_3^2 + k_1^2 k_3^2 &= \frac{3(3n+5)}{n+1},
\end{aligned}$$

where $n \in \{3, 6, 12, 24\}$.

(iv) If $g = 4$, according to (4) and (7) of Lemma 4.1, we obtain $m_1 = m_3$, $m_2 = m_4$. Furthermore, the specific relationships between the principal curvatures can be expressed as

$$k_2 = \frac{k_1 - 1}{k_1 + 1}, \quad k_3 = -\frac{1}{k_1}, \quad k_4 = -\frac{k_1 + 1}{k_1 - 1}.$$

Denote

$$A = k_1 + k_3, \quad B = k_2 + k_4.$$

Then

$$\begin{aligned}
S_1 &= m_1 A + m_2 B; \\
S_n &= k_1^{m_1} k_2^{m_2} k_3^{m_3} k_4^{m_4} = (-1)^{m_1+m_2}, \\
S_{n-1} &= S_n \left(\frac{m_1}{k_1} + \frac{m_2}{k_2} + \frac{m_3}{k_3} + \frac{m_4}{k_4} \right) = (-1)^{m_1+m_2+1} S_1,
\end{aligned}$$

and

$$S_{n-1} - (n+1)S_1 S_n = S_1 \left((-1)^{m_1+m_2+1} - (n+1)(-1)^{m_1+m_2} \right) = 0.$$

Then we attain

$$S_1 = m_1 A + m_2 B = 0.$$

It is noteworthy that $AB = -4$, and from this, we derive

$$A^2 = \frac{4m_2}{m_1}.$$

The fact that $n = 2(m_1 + m_2)$ is an even number necessitates the condition $S_n = (-1)^{m_1+m_2} > 0$, which in turn implies that $m_1 + m_2$ must be an even number. Applying (4) of Lemma 4.1, we deduce that $m_1 = m_2 = 2$, resulting in $n = 8$. Subsequently, the specific values of the principal curvatures can be determined as

$$k_1 = 1 + \sqrt{2}, \quad k_2 = \sqrt{2} - 1, \quad k_3 = 1 - \sqrt{2}, \quad k_4 = -(1 + \sqrt{2}),$$

(v) If $g = 6$, by (6) of Lemma 4.1, we deduce that $m_1 = \dots = m_6$ can only take values of 1 or 2. Further, based on part (7) of the same lemma, we have the following expressions

$$\begin{aligned} k_1 = \cot \theta, \quad k_2 = \frac{\sqrt{3}k_1 - 1}{k_1 + \sqrt{3}}, \quad k_3 = \frac{k_1 - \sqrt{3}}{1 + \sqrt{3}k_1}, \\ k_4 = -\frac{1}{k_1}, \quad k_5 = -\frac{1}{k_2}, \quad k_6 = -\frac{1}{k_3}. \end{aligned}$$

Using these values, we can express the sums as follows

$$S_1 = m_1 \sum_{i=1}^6 k_i, \quad S_n = 1, \quad S_{n-1} = -m_1 S_1,$$

and

$$S_{n-1} - (n+1)S_1 S_n = S_1(-m_1 - (6m_1 + 1)) = 0.$$

Then $S_1 = 0$ results in

$$\begin{aligned} k_1 = 2 + \sqrt{3}, \quad k_2 = 1, \quad k_3 = 2 - \sqrt{3}, \\ k_4 = -(2 - \sqrt{3}), \quad k_5 = -1, \quad k_6 = -(2 + \sqrt{3}). \end{aligned}$$

We exclude the case where $n = 6$ due to the fact that $S_6 = -1 < 0$.

Accordingly, the proof is now comprehensively established, thereby concluding our argument. \square

Remark 4.4. Among these isoparametric equi-centro-affine extremal hypersurfaces outlined in Theorem 4.3, the hypersurfaces specified in (ii) with the condition $2m = n$, as well as those in (iv) and (v) are Euclidean isoparametric minimal hypersurfaces in $\mathbb{S}^{n+1}(1)$. In addition, the hypersurfaces in (iv) and (v) are isoparametric Willmore hypersurfaces.

Theorem 4.5. *Let M^n be a compact equi-centro-affine extremal hypersurface in unit sphere \mathbb{S}^{n+1} . Consequently, the ensuing conclusions hold true.*

- If $0 < k_i \leq \frac{1}{\sqrt{n+1}}$, $i = 1, \dots, n$, then M^n is a totally umbilic hypersphere with $k_i = \frac{1}{\sqrt{n+1}}$, $i = 1, \dots, n$.

- If $k_i \geq \frac{1}{\sqrt{n+1}}$, $i = 1, \dots, n$, then M^n is a totally umbilic hypersphere with $k_i = \frac{1}{\sqrt{n+1}}$, $i = 1, \dots, n$.

Proof. Pursuant to Proposition B as outlined in [39], we see the Newton tensors are divergence-free, explicitly denoted as $T_r^{ij} = 0$. Thus,

$$\begin{aligned} 0 &= \int_M T_{n-1}^{ij} \nabla_{e_i} \nabla_{e_j} \left(S_n^{-\frac{n+1}{n+2}} \right) + S_n^{-\frac{n+1}{n+2}} (S_{n-1} - (n+1)S_n S_1) d\mu_M \\ &= \int_M S_n^{-\frac{n+1}{n+2}} (S_{n-1} - (n+1)S_n S_1) d\mu_M \\ &= \int_M S_n^{\frac{1}{n+2}} \sum_{i=1}^n \frac{1 - (n+1)k_i^2}{k_i} d\mu_M. \end{aligned}$$

Since $S_n \neq 0$ throughout M^n , the aforementioned formula yields the anticipated outcomes as desired. \square

5. THE CLOSED EQUI-CENTRO-AFFINE EXTREMAL CURVES ON SPHERE

In this section, we undertake a comprehensive classification of closed curves residing on the sphere that fulfill the intricate equation

$$B_{ss} - 2B^{-2} + R^{-2}B = \frac{C_1}{2}, \quad (5.1)$$

where $B = \kappa_g^{-\frac{2}{3}}$ and C_1 is constant. It is noteworthy that this equation holds a pivotal position in characterizing the critical points of equi-centro-affine arc length, subject to the constraint of a fixed enclosed area on the spherical surface. By categorizing these curves, we gain an understanding of their geometric properties, their relationship to arc length metrics, and how they are influenced by the inherent constraints of the spherical geometry.

Definition 5.1. On the sphere S^2 , a curve whose geodesic curvature satisfies (5.1) is called *generalized equi-centro-affine extremal curve*. In particular, if $C_1 \equiv 0$, it is called *equi-centro-affine extremal curve*.

Upon integrating (5.1), we arrive at the subsequent equation, which includes the integration constant C_2 .

$$B_s^2 = C_2 - \frac{B^2}{R^2} - 4B^{-1} + C_1 B. \quad (5.2)$$

Notice that, from the preceding equation, we derive the following crucial inequality

$$C_2 \geq \left(\frac{B}{R} - \frac{RC_1}{2} \right)^2 + 4B^{-1} - \frac{R^2 C_1^2}{4} > -\frac{R^2 C_1^2}{4}.$$

Given the assumption that B is not constant, we now proceed to analyze the solutions of the polynomial equation $B^3 - R^2 C_1 B^2 - R^2 C_2 B + 4R^2 = 0$.

Proposition 5.2. *The polynomial equation $B^3 - \mu B^2 - \lambda B + 4R^2 = 0$, where $\mu = R^2 C_1$ and $\lambda = R^2 C_2$, admits two distinct positive solutions provided that either of the following two conditions is fulfilled:*

(a) *If $\mu \geq -3(2R)^{\frac{2}{3}}$, then*

$$\lambda > \frac{-\mu^2 - (Y_1^{1/3} + Y_2^{1/3})}{12},$$

where $Y_{1,2} = \mu^6 + 2160R^2\mu^3 - 93312R^4 \pm 48\sqrt{3}R\sqrt{(\mu^3 + 108R^2)^3}$.

(b) *If $\mu \leq -3(2R)^{\frac{2}{3}}$, then*

$$\lambda > \frac{-\mu^2}{12} + \frac{\sqrt{\mu(\mu^3 - 864R^2)}}{6} \cos \frac{\vartheta - \pi}{3},$$

where $\vartheta = \arccos \frac{-\mu^6 - 2160R^2\mu^3 + 93312R^4}{\mu(864R^2 - \mu^3)\sqrt{\mu(\mu^3 - 864R^2)}}$.

Proof. Given that $B^3 - \mu B^2 - \lambda B + 4R^2 = 0$ possesses two distinct positive solutions, upon differentiating and analyzing the resulting quadratic equation $3B^2 - 2\mu B - \lambda = 0$, it becomes evident that this quadratic cannot admit two negative roots. Consequently, if $\mu \leq 0$, then it is imperative that $\lambda > 0$ holds true. Concurrently, the fact that $B^3 - \mu B^2 - \lambda B + 4R^2 = 0$ admits three distinct real solutions directly implies the discriminant

$$\Delta = -3(4\lambda^3 + \mu^2\lambda^2 + 72\mu R^2\lambda + 16\mu^3 R^2 - 432R^4) < 0.$$

Now, let us shift our focus to considering the inequality $4\lambda^3 + \mu^2\lambda^2 + 72\mu R^2\lambda + 16\mu^3 R^2 - 432R^4 > 0$. To gain insight, we commence by analyzing the roots of $4\lambda^3 + \mu^2\lambda^2 + 72\mu R^2\lambda + 16\mu^3 R^2 - 432R^4 = 0$. Direct computations yield the coefficients

$$\begin{aligned} \bar{A} &= \mu(\mu^3 - 864R^2), \\ \bar{B} &= -72R^2(7\mu^3 - 216R^2), \\ \bar{C} &= -48R^2\mu^2(\mu^3 - 135R^2) \end{aligned}$$

along with the discriminant

$$\Delta_{\Delta} = \bar{B}^2 - 4\bar{A}\bar{C} = 192R^2(\mu^3 + 108R^2)^3.$$

It is immediately apparent that \bar{A} and \bar{B} cannot simultaneously be zero. Consequently, we proceed with the following three distinct cases based on the behavior of these coefficients and the discriminant.

Case 1. If $\Delta_{\Delta} < 0$, which translates to $\mu^3 < -108R^2$, then the equation $4\lambda^3 + \mu^2\lambda^2 + 72\mu R^2\lambda + 16\mu^3 R^2 - 432R^4 = 0$ possesses three distinct real roots, denoted as λ_1, λ_2 and λ_3 , satisfying the ordering $\lambda_1 < \lambda_2 < 0 < \lambda_3$. By previous statement (if $\mu < 0$, then $\lambda > 0$), $4\lambda^3 + \mu^2\lambda^2 + 72\mu R^2\lambda + 16\mu^3 R^2 - 432R^4 > 0$ yields

$$\lambda > \lambda_3 = \frac{-\mu^2}{12} + \frac{\sqrt{\mu(\mu^3 - 864R^2)}}{6} \cos \frac{\theta - \pi}{3},$$

where $\theta = \arccos \frac{-\mu^6 - 2160R^2\mu^3 + 93312R^4}{\mu(864R^2 - \mu^3)\sqrt{\mu(\mu^3 - 864R^2)}}$.

Case 2. If $\Delta_\Delta < 0$, which signifies that $\mu^3 > -108R^2$, then the equation $4\lambda^3 + \mu^2\lambda^2 + 72\mu R^2\lambda + 16\mu^3R^2 - 432R^4 = 0$ admits a unique real root, labeled λ_1 , accompanied by a conjugate pair of complex roots, λ_2 and λ_3 . The real root can be expressed as

$$\lambda_1 = \frac{-\mu^2 - (Y_1^{1/3} + Y_2^{1/3})}{12},$$

where

$$Y_{1,2} = \mu^6 + 2160R^2\mu^3 - 93312R^4 \pm 48\sqrt{3}R\sqrt{(\mu^3 + 108R^2)^3}.$$

Employing the relationship among the roots of the cubic equation, specifically $\lambda_1\lambda_2\lambda_3 = -\frac{16\mu^3R^2 - 432R^4}{4}$, and recognizing that $\mu \leq 0$ leads to $\lambda_1 > 0$ (in accordance with the previously established conditions), we can conclude that for $4\lambda^3 + \mu^2\lambda^2 + 72\mu R^2\lambda + 16\mu^3R^2 - 432R^4 > 0$ to hold, it is necessary that

$$\lambda > \frac{-\mu^2 - (Y_1^{1/3} + Y_2^{1/3})}{12}.$$

Case 3. If $\Delta_\Delta = 0$, that is $\mu^3 = -108R^2$, the equation $4\lambda^3 + \mu^2\lambda^2 + 72\mu R^2\lambda + 16\mu^3R^2 - 432R^4 = 0$ possesses three distinct real solutions, denoted as $\lambda_1, \lambda_2, \lambda_3$, and

$$\lambda_1 = \frac{15}{2^{2/3}}R^{4/3}, \quad \lambda_2 = \lambda_3 = -3(2R)^{4/3}.$$

In this scenario, for $4\lambda^3 + \mu^2\lambda^2 + 72\mu R^2\lambda + 16\mu^3R^2 - 432R^4 > 0$ to hold true, it is necessary that

$$\lambda > \frac{15}{2^{2/3}}R^{4/3}.$$

Notably, this result is consistent with and encompasses the conclusions drawn from the previous cases (Case 1 and Case 2) when the condition $\mu^3 = -108R^2$ is imposed. \square

Remark 5.3. In Figure 1, we illustrate the ranges for C_1 and C_2 as specified by Proposition 5.2, taking into account various values of R . These curves depicted in the figure intersect the C_1 axis at $C_1 = 3R^{-4/3}$ and touch the C_2 axis at $C_2 = 3(2/R)^{2/3}$. This visualization provides a clear understanding of how the ranges for C_1 and C_2 vary with different values of R , as prescribed by the proposition.

Theorem 5.4. *Suppose that $\frac{B^3}{R^2} - C_1B^2 - C_2B + 4 = 0$ admits two distinct positive roots, denoted as A_1 and A_2 , with $A_1 > A_2$. Then, the progression*

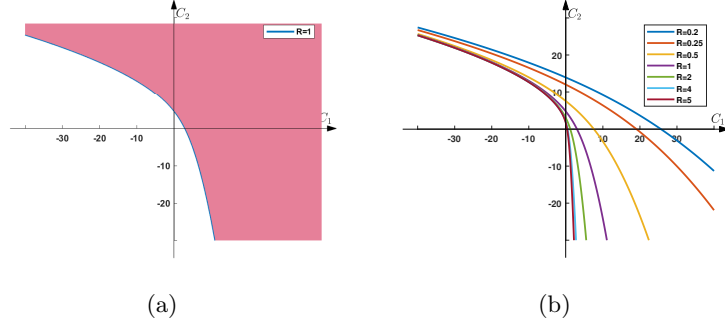


FIGURE 1. The ranges for C_1 and C_2 determined by Proposition 5.2.

angle Λ^Θ within one period of the curvature can be expressed as follows

$$2\sqrt{\frac{4C_2}{R^2} + C_1^2} \int_{A_2}^{A_1} \frac{B^{-\frac{1}{2}}}{(C_2 - B^2/R^2 + C_1B)\sqrt{C_2 - B^2/R^2 - 4B^{-1} + C_1B}} dB.$$

Proof. It is straightforward to observe that within one period, the arc length T is given by

$$T = 2 \int_{A_2}^{A_1} \frac{1}{\sqrt{C_2 - B^2/R^2 - 4B^{-1} + C_1B}} dB$$

after utilizing (5.2). Furthermore, by combining equations (5.1) and (3.7), we discover

$$\mathbf{J} = -2B^{-\frac{1}{2}}\mathbf{T} + B_s\boldsymbol{\epsilon}$$

constitutes a Killing vector field along the curve \mathbf{x} . Now we can employ the spherical coordinates $\mathbf{x}(\theta, \psi) = R(\cos \psi, \cos \theta \sin \psi, \sin \theta \sin \psi)$, so that its equator gives the only integral geodesic of $\mathbf{J} : \mathbf{x}_\theta = b\mathbf{J}$, which generates

$$\mathbf{x}_\theta^2 = R^2 \sin^2 \psi = b^2(4B^{-1} + B_s^2).$$

From the definition of the tangent vector, we have

$$\mathbf{T} = \mathbf{x}_\theta \frac{d\theta}{ds} + \mathbf{x}_\psi \frac{d\psi}{ds}.$$

Taking the inner product gives

$$\langle \mathbf{T}, \mathbf{x}_\theta \rangle = \langle \mathbf{x}_\theta, \mathbf{x}_\theta \rangle \frac{d\theta}{ds} = R^2 \sin^2 \psi \frac{d\theta}{ds}.$$

Substituting the expression for \mathbf{J} from earlier, and using the relationship between \mathbf{T} and \mathbf{x}_θ , we derive

$$\frac{d\theta}{ds} = \frac{\langle \mathbf{T}, \mathbf{x}_\theta \rangle}{R^2 \sin^2 \psi} = \frac{-2B^{-\frac{1}{2}}}{b(4B^{-1} + B_s^2)} = \frac{-2B^{-\frac{1}{2}}}{b(C_2 - B^2/R^2 + C_1B)}$$

and

$$\Lambda^\Theta = \int_0^T \frac{2\sqrt{B^{-1}}}{b(C_2 - B^2/R^2 + C_1B)} ds. \quad (5.3)$$

Let $\bar{\mathbf{x}}$ denote the integral curve of vector field $\bar{\mathbf{T}} = \frac{\mathbf{J}}{|\mathbf{J}|}$. Specifically,

$$\bar{\mathbf{T}} = \frac{1}{\sqrt{C_2 - B^2/R^2 + C_1B}} (-2B^{-\frac{1}{2}}\mathbf{T} + B_s\boldsymbol{\epsilon}).$$

Therefore at the point where $B_s = 0$, we need to find the derivative

$$\begin{aligned} \bar{\mathbf{T}}_{\bar{s}} = \frac{ds}{d\bar{s}} \left(\frac{-2B^{-\frac{1}{2}}}{\sqrt{C_2 - B^2/R^2 + C_1B}} (B^{-\frac{3}{2}}\boldsymbol{\epsilon} - \frac{1}{R^2}\mathbf{x}) \right. \\ \left. + \frac{B_{ss}}{\sqrt{C_2 - B^2/R^2 + C_1B}} \boldsymbol{\epsilon} \right). \end{aligned}$$

At that given point, we have $\mathbf{x} = \bar{\mathbf{x}}$, which implies

$$\frac{ds}{d\bar{s}} = \frac{\sqrt{C_2 - B^2/R^2 + C_1B}}{-2B^{-\frac{1}{2}}}.$$

Accordingly,

$$|\bar{\mathbf{T}}_{\bar{s}}| = \sqrt{\frac{(B_{ss} - 2B^{-2})^2}{4B^{-1}} + \frac{1}{R^2}},$$

which is the curvature of $\bar{\mathbf{x}}$ at the point. Since $\bar{\mathbf{x}}$ represents a planar circle, its curvature is equivalently expressed as the reciprocal of the radius. Thus

$$\frac{1}{|\mathbf{x}_\theta|} = \sqrt{\frac{(B_{ss} - 2B^{-2})^2}{4B^{-1}} + \frac{1}{R^2}}$$

which generates

$$\frac{1}{b} = \sqrt{\frac{C_2}{R^2} + \frac{C_1^2}{4}}.$$

Incorporating this into (5.3) results in the anticipated outcome. \square

In light of the identity

$$\begin{aligned} \frac{1}{C_2 - B^2/R^2 + C_1B} &= \frac{1}{2} \left(C_2 + \left(\frac{RC_1}{2} \right)^2 \right)^{-1/2} \times \\ &\left(\left(\sqrt{C_2 + \left(\frac{RC_1}{2} \right)^2} - \left(\frac{B}{R} - \frac{RC_1}{2} \right) \right)^{-1} \right. \\ &\left. + \left(\sqrt{C_2 + \left(\frac{RC_1}{2} \right)^2} + \left(\frac{B}{R} - \frac{RC_1}{2} \right) \right)^{-1} \right), \end{aligned}$$

we observe that

$$\begin{aligned} \Lambda^\Theta &= \frac{2}{\sqrt{R}} \int_{\tilde{A}_2}^{\tilde{A}_1} \frac{d\tilde{B}}{(r - \tilde{B})\sqrt{(\tilde{A}_1 - \tilde{B})(\tilde{B} - \tilde{A}_2)(\tilde{B} - \tilde{A}_3)}} \\ &\quad + \frac{2}{\sqrt{R}} \int_{\tilde{A}_2}^{\tilde{A}_1} \frac{d\tilde{B}}{(r + \tilde{B})\sqrt{(\tilde{A}_1 - \tilde{B})(\tilde{B} - \tilde{A}_2)(\tilde{B} - \tilde{A}_3)}}, \end{aligned} \quad (5.4)$$

where $r = \sqrt{C_2 + \left(\frac{RC_1}{2}\right)^2}$, $\tilde{B} = \frac{B}{R} - \frac{RC_1}{2}$, and $\tilde{A}_i = \frac{A_i}{R} - \frac{RC_1}{2}$ ($i = 1, 2, 3$). Additionally, the expressions of A_1, A_2 and A_3 can be derived as follows

$$\begin{aligned} \theta &= \arccos \frac{108 - 9C_1C_2R^2 - 2C_1^3R^4}{2R(C_1^2R^2 + 3C_2)^{3/2}}, \\ A_1 &= \frac{C_1R^2}{3} + \frac{2R}{3} \sqrt{C_1^2R^2 + 3C_2} \cos \frac{\theta - \pi}{3}, \\ A_2 &= \frac{C_1R^2}{3} + \frac{2R}{3} \sqrt{C_1^2R^2 + 3C_2} \cos \frac{\theta + \pi}{3}, \\ A_3 &= \frac{C_1R^2}{3} - \frac{2R}{3} \sqrt{C_1^2R^2 + 3C_2} \cos \frac{\theta}{3}. \end{aligned}$$

Let D denote the lower bounds of λ as specified in Proposition 5.2. Notably, θ exhibits a monotonic increase with respect to λ , and its limiting behavior is characterized by

$$\lim_{\lambda \rightarrow D} \theta = 0, \quad \lim_{\lambda \rightarrow +\infty} \theta = \frac{\pi}{2}. \quad (5.5)$$

For the sake of brevity and clarity, we introduce the notations

$$\begin{aligned} d &= \sqrt{C_1^2R^2 + 3C_2}, \\ a &= \frac{2}{3}d \cos \frac{\theta - \pi}{3} - \frac{RC_1}{6}, \\ b &= \frac{2}{3}d \cos \frac{\theta + \pi}{3} - \frac{RC_1}{6}, \\ c &= -\frac{2}{3}d \cos \frac{\theta}{3} - \frac{RC_1}{6}, \end{aligned}$$

which exhibit the subsequent characteristics.

Lemma 5.5. *a, r, d is monotonically increasing and b, c is monotonically decreasing with respect to C_2 . moreover, $a > b > c$ and $r > b$.*

Lemma 5.6. *The limits stated below are valid.*

$$\lim_{\lambda \rightarrow +\infty} \frac{a}{r} = 1, \quad \lim_{\lambda \rightarrow +\infty} \frac{c}{a} = -1, \quad \lim_{\lambda \rightarrow +\infty} \frac{b}{a} = 0, \quad \lim_{\lambda \rightarrow +\infty} a^2(r - a)R = 2.$$

Upon performing a series expansion centered at $x = 0$ with the parameter $x = 1/(d + 1)$, we establish

Lemma 5.7. $\frac{(a-b)(c-r)}{(a-c)(b-r)}$ is monotonically increasing with respect to C_2 , and furthermore, $\frac{(a-b)(c-r)}{(a-c)(b-r)} < 1$.

Based on [25], we obtain an elegant expression for the given integral

$$\int_b^a \frac{d\tilde{B}}{(r+\tilde{B})\sqrt{(a-\tilde{B})(\tilde{B}-b)(\tilde{B}-c)}} = \frac{2}{(a+r)\sqrt{a-c}} \Pi\left(\frac{a-b}{a+r}, \frac{\pi}{2}, \frac{a-b}{a-c}\right),$$

where Π denotes the elliptic integral of the third kind defined as follows

$$\begin{aligned} \Pi(n, \varphi, m) &= \int_0^\varphi \frac{d\theta}{(1-n\sin^2\theta)\sqrt{1-m\sin^2\theta}} \\ &= \int_0^{\sin\varphi} \frac{dt}{(1-nt^2)\sqrt{(1-mt^2)(1-t^2)}}. \end{aligned}$$

Utilizing Lemma 5.5, we confirm that $r > b$ holds for all R, C_1 and C_2 . Further, drawing from [25], we express the given integral as

$$\begin{aligned} \int_b^a \frac{d\tilde{B}}{(r-\tilde{B})\sqrt{(a-\tilde{B})(\tilde{B}-b)(\tilde{B}-c)}} &= \frac{-2(c-b)}{(c-r)(b-r)\sqrt{a-c}} \times \\ &\quad \Pi\left(\frac{(a-b)(c-r)}{(a-c)(b-r)}, \frac{\pi}{2}, \frac{a-b}{a-c}\right) \\ &\quad + \frac{-2}{(c-r)\sqrt{a-c}} \Pi\left(0, \frac{\pi}{2}, \frac{a-b}{a-c}\right). \end{aligned}$$

Subsequently, we derive the refined form of Λ^Θ ,

$$\begin{aligned} \Lambda^\Theta &= \frac{4}{(a+r)\sqrt{R(a-c)}} \Pi\left(\frac{a-b}{a+r}, \frac{\pi}{2}, \frac{a-b}{a-c}\right) \\ &\quad + \frac{4(b-c)}{(r-c)(r-b)\sqrt{R(a-c)}} \Pi\left(\frac{(a-b)(c-r)}{(a-c)(b-r)}, \frac{\pi}{2}, \frac{a-b}{a-c}\right) \quad (5.6) \\ &\quad + \frac{4}{(r-c)\sqrt{R(a-c)}} \Pi\left(0, \frac{\pi}{2}, \frac{a-b}{a-c}\right). \end{aligned}$$

Proposition 5.8. As $\lambda \rightarrow D$, the limit Λ^Θ of is given by

$$\begin{aligned} \lim_{\lambda \rightarrow D} \Lambda^\Theta &= \frac{12\pi}{\sqrt{Rd_0}} \left(\frac{1}{2d_0 + 6r_0 - RC_1} + \frac{1}{6r_0 + 4d_0 + RC_1} \right. \\ &\quad \left. + \frac{6d_0}{(6r_0 + 4d_0 + RC_1)(6r_0 - 2d_0 + RC_1)} \right), \end{aligned}$$

where $r_0 = \sqrt{\frac{D}{R^2} + \frac{R^2C_1^2}{4}}$ and $d_0 = \sqrt{\frac{3D}{R^2} + C_1^2R^2}$, with D being the lower bound of λ in Proposition 5.2.

Proof. Observe that

$$\begin{aligned} \lim_{\lambda \rightarrow D} r = r_0, \quad \lim_{\lambda \rightarrow D} d = d_0, \quad \lim_{\lambda \rightarrow D} c = -\frac{2d_0}{3} - \frac{RC_1}{6}, \\ \lim_{\lambda \rightarrow D} a = \lim_{\lambda \rightarrow D} b = \frac{d_0}{3} - \frac{RC_1}{6}. \end{aligned}$$

Substituting these limits into the expression (5.6) and simplifying the resulting terms, we directly obtain the stated result. \square

Proposition 5.9. *The following limit holds true:*

$$\lim_{\lambda \rightarrow +\infty} \Lambda^\Theta = \pi.$$

Proof. According to Lemma 5.6, it is immediately evident that

$$\lim_{\lambda \rightarrow +\infty} \frac{4}{(a+r)\sqrt{R(a-c)}} \Pi\left(\frac{a-b}{a+r}, \frac{\pi}{2}, \frac{a-b}{a-c}\right) = 0$$

and similarly,

$$\lim_{\lambda \rightarrow +\infty} \frac{4}{(r-c)\sqrt{R(a-c)}} \Pi\left(0, \frac{\pi}{2}, \frac{a-b}{a-c}\right) = 0.$$

Now, let us focus our attention to the remaining component within (5.6). Supposing that

$$\alpha^2 = \frac{(a-b)(c-r)}{(a-c)(b-r)}, \quad k^2 = \frac{a-b}{a-c},$$

we may readily observe that

$$\lim_{\lambda \rightarrow +\infty} \alpha^2 = 1, \quad \lim_{\lambda \rightarrow +\infty} k^2 = \frac{1}{2}.$$

According to [13], we obtain the expansion

$$\begin{aligned} \int_0^{\frac{\pi}{2}} \frac{d\theta}{(1-\alpha^2 \sin^2 \theta)\sqrt{1-k^2 \sin^2 \theta}} &= \int_0^{\frac{\pi}{2}} \frac{d\theta}{\sqrt{1-k^2 \sin^2 \theta}} \\ &+ \frac{1}{1-k^2} \int_0^{\frac{\pi}{2}} \sqrt{1-k^2 \sin^2 \theta} d\theta \\ &+ \frac{(2-k^2(1+\alpha^2))\pi}{4(1-k^2)\sqrt{1-k^2}\sqrt{1-\alpha^2}} \\ &+ o(1-\alpha^2), \end{aligned}$$

where $\alpha^2 \neq 1$ and $o(1-\alpha^2)$ signifies that the remaining terms are bounded by $(1-\alpha^2)C$ for some constant C . One can verify that

$$\lim_{k^2 \rightarrow \frac{1}{2}} \int_0^{\frac{\pi}{2}} \frac{d\theta}{\sqrt{1-k^2 \sin^2 \theta}} = 0, \quad \lim_{k^2 \rightarrow \frac{1}{2}} \int_0^{\frac{\pi}{2}} \sqrt{1-k^2 \sin^2 \theta} d\theta = 0.$$

Direct computation shows

$$\lim_{\lambda \rightarrow +\infty} \frac{4(b-c)}{(r-c)(r-b)\sqrt{R(a-c)}\sqrt{1-\alpha^2}} = \sqrt{2},$$

and

$$\lim_{\lambda \rightarrow +\infty} \frac{(2-k^2(1+\alpha^2))}{4(1-k^2)\sqrt{1-k^2}} = \frac{\sqrt{2}}{2}.$$

Given these limits, it is direct to deduce the desired result. \square

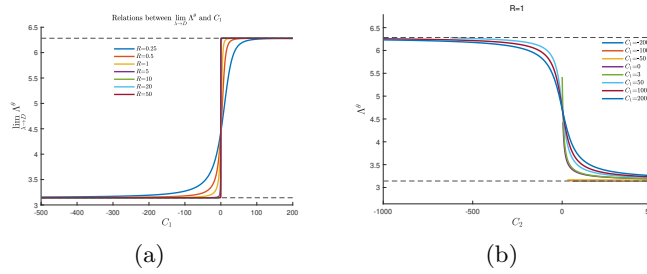


FIGURE 2. The incremental or decremental processes of Λ^Θ .

Fig. 2 presents a comprehensive visualization showcasing the varying trends of the progression angle Λ^Θ , contingent upon diverse variables and inputs. Specifically, Fig. 2 (a), by modulating the parameter R , it becomes evident that $\lim_{\lambda \rightarrow D} \Lambda^\Theta$ exhibits a monotonic increase with respect to C_1 . Additionally, two notable limits can be discerned: $\lim_{C_1 \rightarrow -\infty} \lim_{\lambda \rightarrow D} \Lambda^\Theta = \pi$ and

$$\lim_{C_1 \rightarrow +\infty} \lim_{\lambda \rightarrow D} \Lambda^\Theta = 2\pi.$$

Utilizing (5.2) for analysis, upon investigation of the consequences of re-sizing the sphere, we ascertain that the scale of the spherical radius R does not influence the fundamental dynamics of the progression angle Λ^Θ . As depicted in Fig. 2 (b), when C_1 is held at different constants, the progression angle Λ^Θ consistently demonstrates a monotonic decrease in response to variations in C_2 . To substantiate this observation, in Appendix B, we provide a rigorous proof of the monotonicity of the progression angle Λ^Θ specifically for the case where $C_1 = 0$ and $R = 1$, serving as an illustrative example. Analogous approaches can be adopted to delve into the intricate behaviors of Λ^Θ under diverse parameter settings and conditions, offering a comprehensive understanding of its dynamic properties across various scenarios. Indeed, we have firmly established the following result.

Proposition 5.10. (1) For $C_1 = 0$, we have $\lim_{\lambda \rightarrow D} \Lambda^\Theta = \sqrt{2}\pi$.

(2) For all R , $\lim_{\lambda \rightarrow D} \Lambda^\Theta$ is monotonic increasing with respect to C_1 , and

$$\lim_{C_1 \rightarrow -\infty} \lim_{\lambda \rightarrow D} \Lambda^\Theta = \pi, \quad \lim_{C_1 \rightarrow +\infty} \lim_{\lambda \rightarrow D} \Lambda^\Theta = 2\pi.$$

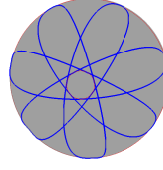
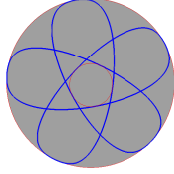
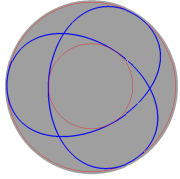
- (3) Holding C_1 and R constant, Λ^Θ is monotonic decreasing with respect to C_2 and $\pi < \Lambda^\Theta < \lim_{\lambda \rightarrow D} \Lambda^\Theta$.
- (4) For all R, C_1, C_2 , the range of Λ^Θ is constrained to $\pi < \Lambda^\Theta < 2\pi$.

Theorem 5.11. *Let \mathbf{x} be a smoothly embedded closed curve residing on a sphere, whose curvatures satisfy the condition stated in (5.1). Then \mathbf{x} is inherently a planar curve. In other words, the smoothly closed and embedded generalized equi-centro-affine extremal curves residing on a sphere are precisely planar circles.*

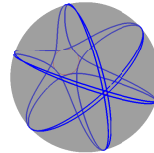
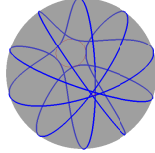
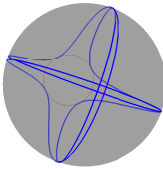
Regarding the classification of closed generalized equi-centro-affine extremal curves on a sphere, we have

Theorem 5.12. *Let \mathbf{x} be a closed generalized equi-centro-affine extremal curve on sphere. Then we have the following possibilities for \mathbf{x} .*

- (1) \mathbf{x} is a planar circle on sphere;
- (2) $\mathbf{x} = \mathbf{x}_{p,q}$, a curve whose curvature is a nonconstant periodic solution of (5.1) depending upon $(p, q) \in \mathbf{N} \times \mathbf{N}$. The pair (p, q) is by no means arbitrary and must be such that p/q is defined to the open interval $\left(1/2, \lim_{\lambda \rightarrow D} \Lambda^\Theta / 2\pi\right)$, where $\lim_{\lambda \rightarrow D} \Lambda^\Theta$ is obtained in Proposition 5.8.



(a) $p = 2, q = 3, C_1 = 0$ (b) $p = 3, q = 5, C_1 = 0$ (c) $p = 4, q = 7, C_1 = 0$



(d) $p = 3, q = 4, C_1 = 20$ (e) $p = 4, q = 5, C_1 = 30$ (f) $p = 5, q = 6, C_1 = 30$

FIGURE 3. The closed extremal curves on unit sphere.

Taking $R = 1$ and $C_1 = 0$ as an illustrative example, we demonstrate the classification of closed generalized equi-centro-affine extremal curves on a sphere, which restricts the ratio p/q to lie within the open interval $(1/2, \sqrt{2}/2)$. To extend this range and obtain closed curves with p/q values

in the interval $(\sqrt{2}/2, 1)$, we can adjust the parameter C_1 to specific values such as $C_1 = 20$ or $C_1 = 30$. As depicted in Fig. 3, several closed curves $\mathbf{x}_{p,q}$ are presented, all of which can be considered as generalized equi-centro-affine extremal curves on the sphere under these parameter settings.

APPENDIX A: SOME CALCULATIONS FOR THEOREM 3.1

In this part, we provide a more detailed exposition of the computation process leading to the derivation of the second variational formula presented in Theorem 3.1. By (3.2), we have

$$\begin{aligned}
& \frac{\partial}{\partial t} \left(S_n^{-\frac{n+1}{n+2}} \left(\frac{1}{\varrho^2} S_{n-1} - (n+1) S_1 S_n \right) \right) \\
&= U_{,ij} \left(-\frac{n+1}{n+2} S_n^{-\frac{2n+3}{n+2}} T_{n-1}^{ij} \left(\frac{1}{\varrho^2} S_{n-1} - (n+1) S_1 S_n \right) \right. \\
&\quad \left. + S_n^{-\frac{n+1}{n+2}} \left(\frac{1}{\varrho^2} T_{n-2}^{ij} - (n+1) (T_0^{ij} S_n + S_1 T_{n-1}^{ij}) \right) \right) \\
&\quad + U \left(-\frac{n+1}{n+2} S_n^{-\frac{2n+3}{n+2}} \left(\frac{1}{\varrho^4} S_{n-1}^2 - (n+1) S_1^2 S_n^2 - \frac{n}{\varrho^2} S_1 S_{n-1} S_n \right) \right. \\
&\quad \left. + S_n^{-\frac{n+1}{n+2}} \left(\frac{2}{\varrho^4} S_{n-2} - \frac{n}{\varrho^2} S_n + 2(n+1) S_2 S_n \right. \right. \\
&\quad \left. \left. - \frac{n(n+1)}{\varrho^2} S_n - 2(n+1) S_1^2 S_n - \frac{n}{\varrho^2} S_1 S_{n-1} \right) \right) \\
&\quad + W^j \left(-\frac{n+1}{n+2} S_n^{-\frac{2n+3}{n+2}} S_{n,j} \left(\frac{1}{\varrho^2} S_{n-1} - (n+1) S_1 S_n \right) \right. \\
&\quad \left. + S_n^{-\frac{n+1}{n+2}} \left(\frac{1}{\varrho^2} S_{n-1,j} - (n+1) (S_{1,j} S_n + S_1 S_{n,j}) \right) \right).
\end{aligned}$$

On the other hand,

$$\frac{\partial}{\partial t} \left(\left(S_n^{-\frac{n+1}{n+2}} \right)_{,ij} T_{n-1}^{ij} \right) = \frac{\partial}{\partial t} \left(\left(S_n^{-\frac{n+1}{n+2}} \right)_{,ij} \right) T_{n-1}^{ij} + \left(S_n^{-\frac{n+1}{n+2}} \right)_{,ij} \frac{\partial}{\partial t} T_{n-1}^{ij},$$

and

$$\begin{aligned}
\frac{\partial}{\partial t} \left(\left(S_n^{-\frac{n+1}{n+2}} \right)_{,ij} \right) &= \bar{\nabla}_{\frac{\partial}{\partial t}} \bar{\nabla}_{e_j} e_i \left(S_n^{-\frac{n+1}{n+2}} \right) - \frac{\partial}{\partial t} \left(\Gamma_{ij}^k e_k \left(S_n^{-\frac{n+1}{n+2}} \right) \right) \\
&= \left(\frac{\partial}{\partial t} \left(S_n^{-\frac{n+1}{n+2}} \right) \right)_{,ij} - \frac{\partial \Gamma_{ij}^k}{\partial t} e_k \left(S_n^{-\frac{n+1}{n+2}} \right) \\
&\quad + \bar{R} \left(e_j, \frac{\partial \mathbf{x}}{\partial t} \right) e_i \left(S_n^{-\frac{n+1}{n+2}} \right).
\end{aligned}$$

According to (3.2), we may find

$$\begin{aligned} \left(\frac{\partial}{\partial t} S_n^{-\frac{n+1}{n+2}}\right)_{,ij} T_{n-1}^{ij} = & A_4 U_{,mkij} + A_3 U_{,mki} + A_2 U_{,mk} + A_1 U_{,m} \\ & + A_0 U + B_2 W_{,ij}^m + B_1 W_{,i}^m + B_0 W^m, \end{aligned}$$

where

$$\begin{aligned} A_4 &= -\frac{n+1}{n+2} S_n^{-\frac{2n+3}{n+2}} T_{n-1}^{mk} T_{n-1}^{ij}, \\ A_3 &= -\frac{2(n+1)}{n+2} \left(S_n^{-\frac{2n+3}{n+1}} T_{n-1}^{mk}\right)_{,j} T_{n-1}^{ij}, \\ A_2 &= -\frac{n+1}{n+2} \left(S_n^{-\frac{2n+3}{n+2}} T_{n-1}^{mk}\right)_{,ij} T_{n-1}^{ij} - \frac{n+2}{n+2} S_n^{-\frac{2n+3}{n+2}} (S_1 S_n + \frac{1}{\varrho^2} S_{n-1}) T_{n-1}^{mk}, \\ A_1 &= -\frac{2(n+1)}{n+2} \left(S_n^{-\frac{2n+3}{n+2}} (S_1 S_n + \frac{1}{\varrho^2} S_{n-1})\right)_k T_{n-1}^{mk}, \\ A_0 &= -\frac{n+1}{n+2} \left(S_n^{-\frac{2n+3}{n+2}} (S_1 S_n + \frac{1}{\varrho^2} S_{n-1})\right)_{,ij} T_{n-1}^{ij}, \\ B_2 &= \left(S_n^{-\frac{n+1}{n+2}}\right)_m T_{n-1}^{ij}, \\ B_1 &= 2 \left(S_n^{-\frac{n+1}{n+2}}\right)_{,mj} T_{n-1}^{ij}, \\ B_0 &= \left(S_n^{-\frac{n+1}{n+2}}\right)_{,mij} T_{n-1}^{ij}. \end{aligned}$$

(3.4), (3.5) and above computations yield Theorem 3.1.

APPENDIX B: MONOTONICITY OF THE PROGRESSION ANGLE

According to (5.2), upon examining the effects of scaling the sphere, we ascertain that the magnitude of the spherical radius R has no impact on the overarching dynamics of the progression angle Λ^Θ . Consequently, a simplifying assumption of $R = 1$ can be safely made without affecting the analysis. Here, we present a meticulous proof of the monotonicity of the progression angle for the specific case where $R = 1$ and $C_1 = 0$, which serves as a prototypical example. It is worth noting that when $C_1 \neq 0$, the progression angle can be expanded as a series in terms of the parameter $x = 1/(d+1)$ around $x = 0$, facilitating further analysis in more complex scenarios. For $R = 1, C_1 = 0$, we have $r > a$, and (5.4) can be rewritten as

$$\begin{aligned} \Lambda^\Theta &= \frac{4}{(a+r)\sqrt{(a-c)}} \Pi\left(\frac{a-b}{a+r}, \frac{\pi}{2}, \frac{a-b}{a-c}\right) \\ &\quad - \frac{4}{(a-r)\sqrt{(a-c)}} \Pi\left(\frac{a-b}{a-r}, \frac{\pi}{2}, \frac{a-b}{a-c}\right). \end{aligned} \tag{B.1}$$

Utilizing the series expansions for the elliptic integral of the third kind, as detailed in the reference [13], under the conditions where $\alpha < -1$, $0 \leq k < 1$ or $0 < \alpha < 1$, $0 \leq k < \alpha$, we can express the elliptic integral as follows:

$$\Pi\left(\alpha, \frac{\pi}{2}, k\right) = \sum_{m=0}^{\infty} c_m k^m, \quad (\text{B.2})$$

where

$$\begin{aligned} c_0 &= \frac{\pi}{2\sqrt{1-\alpha}}, \quad c_1 = \frac{\pi}{4\alpha} \left(\frac{1}{\sqrt{1-\alpha}} - 2 \right), \\ c_2 &= \frac{3\pi}{32\alpha^2} \left(\frac{2}{\sqrt{1-\alpha}} - 2 - \alpha \right), \\ c_3 &= \frac{5\pi}{256\alpha^3} \left(-4\alpha - 3\alpha^2 - 8 + \frac{8}{\sqrt{1-\alpha}} \right), \\ 2(m+1)\alpha c_{m+1} &= \frac{\pi}{2(2m-1)} \left(\frac{-\frac{1}{2}}{m} \right)^2 + (1-2m)c_{m-1} + (2m+1+2m\alpha)c_m. \end{aligned}$$

For the first part of Λ^Θ , i.e., $\frac{4}{(a+r)\sqrt{(a-c)}}\Pi\left(\frac{a-b}{a+r}, \frac{\pi}{2}, \frac{a-b}{a-c}\right)$, we derive

$$\begin{aligned} \frac{4c_0}{(a+r)\sqrt{a-c}} &= \pi r^{-\frac{3}{2}} - \frac{3\pi}{2}r^{-\frac{9}{2}} + \frac{79\pi}{8}r^{-\frac{15}{2}} + O(r^{-\frac{21}{2}}), \\ \frac{4c_1}{(a+r)\sqrt{a-c}} \left(\frac{a-b}{a-c} \right) &= \frac{(2-\sqrt{2})\pi}{4}r^{-\frac{3}{2}} - \frac{5\pi}{4}r^{-\frac{9}{2}} \\ &\quad + \frac{115-36\sqrt{9}}{16}\pi r^{-\frac{15}{2}} + O(r^{-\frac{21}{2}}), \\ \frac{4c_2}{(a+r)\sqrt{a-c}} \left(\frac{a-b}{a-c} \right)^2 &= \frac{(24-15\sqrt{2})\pi}{64}r^{-\frac{3}{2}} - \frac{(42-15\sqrt{2})\pi}{32}r^{-\frac{9}{2}} \\ &\quad + \frac{477-171\sqrt{2}}{64}\pi r^{-\frac{15}{2}} + O(r^{-\frac{21}{2}}), \\ \frac{4c_3}{(a+r)\sqrt{a-c}} \left(\frac{a-b}{a-c} \right)^3 &= \frac{5(64-43\sqrt{2})\pi}{1024}r^{-\frac{3}{2}} - \frac{5(72-39\sqrt{2})\pi}{256}r^{-\frac{9}{2}} \\ &\quad + \frac{5(1688-791\sqrt{2})}{1024}\pi r^{-\frac{15}{2}} + O(r^{-\frac{21}{2}}). \end{aligned}$$

For the second part of Λ^Θ , that is, $\frac{-4}{(a-r)\sqrt{(a-c)}}\Pi\left(\frac{a-b}{a-r}, \frac{\pi}{2}, \frac{a-b}{a-c}\right)$, we see

$$\begin{aligned} \frac{-4c_0}{(a-r)\sqrt{a-c}} &= \pi + \frac{\pi}{2}r^{-3} + \frac{11\pi}{8}r^{-6} + O(r^{-9}), \\ \frac{-4c_1}{(a-r)\sqrt{a-c}} \left(\frac{a-b}{a-c} \right) &= \frac{\sqrt{2}\pi}{4}r^{-\frac{3}{2}} - \frac{\pi}{2}r^{-3} - \frac{7\pi}{4}r^{-6} \end{aligned}$$

$$\begin{aligned}
& + \frac{9\sqrt{2}}{4}\pi r^{-\frac{15}{2}} + O(r^{-9}), \\
\frac{-4c_2}{(a-r)\sqrt{a-c}} \left(\frac{a-b}{a-c}\right)^2 &= \frac{3\sqrt{2}\pi}{64}r^{-\frac{3}{2}} - \frac{15\sqrt{2}\pi}{32}r^{-\frac{9}{2}} + \frac{3\pi}{8}r^{-6} \\
& - \frac{9\sqrt{2}}{64}\pi r^{-\frac{15}{2}} + O(r^{-9}), \\
\frac{-4c_3}{(a-r)\sqrt{a-c}} \left(\frac{a-b}{a-c}\right)^3 &= \frac{15\sqrt{2}\pi}{1024}r^{-\frac{3}{2}} - \frac{55\sqrt{2}\pi}{256}r^{-\frac{9}{2}} \\
& - \frac{955\sqrt{2}}{1024}\pi r^{-\frac{15}{2}} + O(r^{-9}).
\end{aligned}$$

Then

$$\begin{aligned}
\Lambda^\Theta &= \pi \left(1 + \frac{280 - 49\sqrt{2}}{128}r^{-\frac{3}{2}} - \frac{350 - 35\sqrt{2}}{64}r^{-\frac{9}{2}} \right. \\
& \left. + \frac{4193 - 735\sqrt{2}}{128}r^{-\frac{15}{2}} \right) + O(r^{-9}). \tag{B.3}
\end{aligned}$$

Then by (B.3) we can easily verify that Λ^Θ is monotonically decreasing when $r > (6\sqrt{3})^{1/3}$, and converges to π as $r \rightarrow +\infty$.

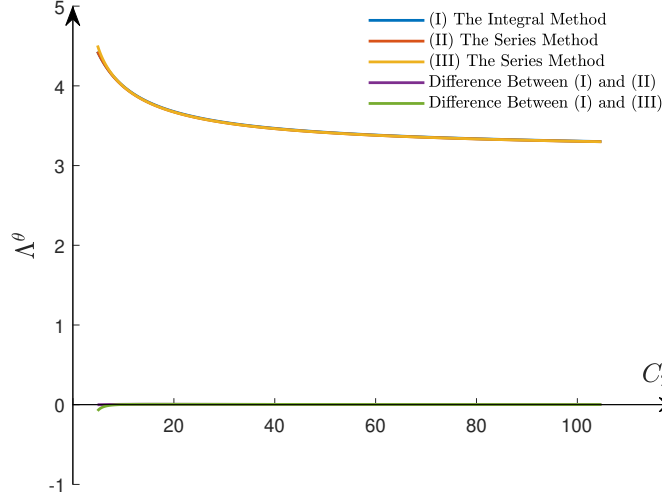


FIGURE 4. The comparison of different method to calculate Λ^Θ .

Remark B.1. In Fig. 4, the curves depicting $\Lambda^\Theta(C_2)$ are precisely rendered using three distinct methods: the numerical integral approach defined in (B.1), the summation of the initial four terms from the series expansion in (B.2), and the approximate series expansions (B.3) with respect to r . Notably, these three representations exhibit remarkable congruence, with minimal deviations among them, essentially indicating a near-perfect overlap.

Acknowledgments. This work was supported by the National NSF of China Grants-12431008.

REFERENCES

- [1] U. ABRESCH, Isoparametric hypersurfaces with four or six distinct principal curvatures, *Math. Ann.*, **264** (1983), 283–302.
- [2] F. J. ALMGREN, Some interior regularity theorems for minimal surfaces and an extension of Bernstein’s theorem, *Ann. Math.*, **84** (1966), 277–292.
- [3] J. ARROYO, O.J. GARAY, J.J. MENCIA, Extremals of curvature energy actions on spherical closed curves, *J. Geom. Phys.*, **51** (2004), 101–125.
- [4] H. BLAINE LAWSON JR, Complete Minimal Surfaces in \mathbb{S}^3 , *Ann. Math.*, **92** (1970), 335–374.
- [5] H. BLAINE LAWSON JR, *Lectures on Minimal Submanifolds, Volume 1*. Publish or Perish, Inc. Berkeley, CA., 1-25, 1980.
- [6] E. BOMBIERI, E. D. GIORGI, E. GIUSTI, Minimal cones and the Bernstein problem, *Invent. Math.*, **7** (1969), 243–268.
- [7] S. BRENDLE, A sharp bound for the area of minimal surfaces in the unit ball, *Geom. Funct. Anal.*, **22** (2012), 621–626.
- [8] S. BRENDLE, Embedded minimal tori in S^3 and the Lawson conjecture, *Acta Math.*, **211** (2013), 177–190.
- [9] S. BRENDLE, Minimal surfaces in \mathbb{S}^3 : a survey of recent results, *Bull. Math. Sci.*, **3** (2013), 133–171.
- [10] S. BRENDLE, The isoperimetric inequality for a minimal submanifold in Euclidean space, *J. Amer. Math. Soc.*, **34** (2021), 595–603.
- [11] S. BRENDLE, Minimal hypersurfaces and geometric inequalities, *Ann. Fac. Sci. Toulouse. Math.*, **32** (2023), 179–201.
- [12] R. BRYANT, A duality theorem for Willmore surfaces, *J. Differential Geom.*, **20** (1984), 23–53.
- [13] P. F. BYARD, M. D. FRIEDMAN, *Handbook of Elliptic Integrals for Engineers and Scientists*, 2nd Edition, Springer-Verlag, Berlin, 1971.
- [14] E. CALABI, Hypersurfaces with maximal affinely invariant area, *Amer. J. Math.*, **104** (1982), 91–126.
- [15] E. CALABI, Affine differential geometry and holomorphic curves, *Lecture Notes Math.*, **1422** (1990), 15–21.
- [16] S.S. CHERN, Affine minimal hypersurfaces, in *Minimal submanifolds and geodesics*, Proc. Japan-United States Sem., Tokyo, 1977, 17–30.
- [17] S.S. CHERN, M. DO CARMO, S. KOBAYASHI, Minimal submanifolds of a sphere with second fundamental form of constant length, *Amer. J. Math.*, **104** (1982), 91–126.
- [18] O. CHODOSH, C. LI, Stable anisotropic minimal hypersurfaces in \mathbb{R}^4 . *Forum Math. Pi* **11** (2023), e3.
- [19] O. CHODOSH, C. LI, Stable minimal hypersurfaces in \mathbb{R}^4 . *Acta Math.*, (2024) To appear.
- [20] T. COLDING, W. MINICOZZI, Shapes of embedded minimal surfaces, *Proc. Nat. Acad. Sciences*, **103**(2006),11106–11111.
- [21] T. COLDING, W. MINICOZZI, *A course in minimal surfaces*, Graduate Studies in Mathematics, 121. American Mathematical Society, Providence, RI, 2011.
- [22] R. COURANT Plateau’s problem and Dirichlet’s principle. *Ann. Math.*, **38**(1937), 679–724.
- [23] J. DOUGLAS, Solution of the problem of Plateau. *Trans. Amer. Math. Soc.*, **33**(1931), 263-321.

- [24] D. FISCHER-COLBRIE, R. SCHOEN, The structure of complete stable minimal surfaces in 3-manifolds of nonnegative scalar curvature, *Comm. Pure Appl. Math.*, **33** (1980), 199–211.
- [25] S. GRADSHTEYN AND I. M. RYZHIK, *Table of Integrals, Series, and Products*, Daniel. Zwillinger and Victor Moll, (eds.), 2014.
- [26] G. HUISKEN, Flow by mean curvature of convex surfaces into spheres, *J. Differential Geom.*, **20** (1984), 237–266.
- [27] J. LANGER, D.A. SINGER, The total squared curvature of closed curves, *J. Differential Geom.*, **20** (1984), 1–22.
- [28] A.M. LI, F. JIA, The Calabi conjecture on affine maximal surfaces, *Results Math.*, **40** (2001), 256–272.
- [29] H. LI, Willmore hypersurfaces in a sphere, *Asian Journal Math.*, **5**(2001), 365–377.
- [30] J. LOFTIN, M. TSUI, Ancient solutions of the affine normal flow, *J. Differential Geom.*, **78** (2008), 113–162.
- [31] F. C. MARQUES, A. NEVES, Min-max theory and the Willmore conjecture, *Ann. of Math.*, **179** (2014), 683–782.
- [32] F. C. MARQUES, A. NEVES, Morse index and multiplicity of min-max minimal hypersurfaces, *Camb. J. Math.*, **4** (2016) 463–511.
- [33] F. C. MARQUES, A. NEVES, Existence of infinitely many minimal hypersurfaces in positive ricci curvature, *Invent. Math.*, (2017) .
- [34] H. F. MUNZNER, Isoparametrische hyperflächen in Sphären I, *Math. Ann.*, **251** (1980), 57–71.
- [35] K. NOMIZU, T. SASAKI, Centroaffine immersions of codimension two and projective hypersurface theory, *Nagoya Math. J.*, **132**(1993), 63–90.
- [36] K. NOMIZU, T. SASAKI, *Affine Differential Geometry: Geometry of Affine Immersions*. Cambridge University Press, 1994.
- [37] P.J. OLVER, C.Z. QU, Y. YANG, Feature matching and heat flow in centroaffine geometry, *Symmetry Integrability Geom. Methods Appl.*, **16** (2020), 093.
- [38] T. RADO, On Plateau’s problem, *Ann. Math.*, **31** (1930), 457–469.
- [39] R. REILLY, Variational properties of functions of the mean curvature for hypersurfaces in space forms, *J. Differential Geom.*, **8** (1973), 465–477.
- [40] R. SCHOEN, L. SIMON, S. T. YAU, Curvature estimates for minimal hypersurfaces, *Acta Math.*, **134** (1975), 275–288.
- [41] J. SIMONS, Minimal varieties in Riemannian manifolds, *Ann. of Math.*, **88** (1968), 62–105.
- [42] U. SIMON, Affine differential geometry [Chapter 9]. In: *Handbook of Differential Geometry*, Vol. 1, pp 905–961, North-Holland, Amsterdam, 2000.
- [43] B. SOLOMON, On the Gauss map of an area-minimizing hypersurface, *J. Differential Geom.*, **19** (1984), 221–232.
- [44] S. STOLZ, Multiplicities of Dupin hypersurfaces, *Invent. Math.*, **138** (1999), 253–279.
- [45] N.S. TRUDINGER, X.J. WANG, The Bernstein problem for affine maximal hypersurfaces, *Invent. Math.*, **140** (2000), 399–422.
- [46] N.S. TRUDINGER, X.J. WANG, Affine complete locally convex hypersurfaces, *Invent. Math.*, **150** (2002), 45–60.
- [47] N.S. TRUDINGER, X.J. WANG, The affine plateau problem, *J. Amer. Math. Soc.*, **18** (2005), 253–289.
- [48] R. WALTER, Centroaffine differential geometry: submanifolds of codimension 2, *Results in Math.*, **13**(1988), 386–402.
- [49] X.J. WANG, Affine maximal hypersurfaces, Proc. ICM, Vol. III, 2002, 221–231.
- [50] Y.Y.L. WANG, On the order of the Euler-Lagrange equations of the variational problem of the affine arc length, *J. Reine Angew Math.*, **245** (1970), 55–62.

- [51] Y.Y.L. WANG, On the solution of the variational problem of the arc length in 4-dimensinal affine space, *J. Reine Angew Math.*, **255** (1972), 99–103.
- [52] W.F. WO, X.L. WANG, C.Z. QU, The centro-affine invariant geometric heat flow, *Math. Z.*, **288** (2018), 311–331.
- [53] Y. YANG, H. LIU, Minimal centroaffine immersions of codimension two, *Results Math.*, **52** (2008), 423–437.
- [54] X. P. ZHU, *Lectures on mean curvature flows*. AMS/IP Studies in Advanced Mathematics, 32, International Press, 2002.

YUN YANG

DEPARTMENT OF MATHEMATICS, NORTHEASTERN UNIVERSITY, SHENYANG, 110819,
P.R. CHINA

Email address, Corresponding author: yangyun@mail.neu.edu.cn

CHANGZHENG QU

SCHOOL OF MATHEMATICS AND STATISTICS, NINGBO UNIVERSITY, NINGBO, 315211,
P.R. CHINA

Email address: quchangzheng@nbu.edu.cn